LRP 396/90 February 1990

INFLUENCE OF TRIANGULARITY AND PLASMA PROFILES ON IDEAL-MHD BETA LIMITS

G. Schultz, A. Bondeson, F. Troyon and A. Roy

INFLUENCE OF TRIANGULARITY AND PLASMA PROFILES ON IDEAL-MHD BETA LIMITS

(Final report, contract 310/88-7 FU CH NET)

G. Schultz, A. Bondeson, F. Troyon, and A. Roy
Centre de Recherches en Physique des Plasmas
Association Euratom - Confédération Suisse
Ecole Polytechnique Fédérale de Lausanne
21 Av. des Bains, CH-1007 Lausanne, Switzerland

Abstract: Ideal-MHD stability calculations are presented to show the effect of triangularity δ on the beta-limit for plasmas of NET/ITER type with ellipticity $\kappa = 2$ and aspect ratio $A = 3.7$. Two different types of beta-optimisations have been made to clarify the influence of the equilibrium profiles. In the first set of optimisations, current profiles that are flat in the central region are prescribed, and the pressure profile is optimised. The resulting pressure profiles are broad and triangularity only has a weak influence on the beta-limit. In the second set, more peaked pressure distributions are prescribed and the current profile is optimised. For peaked pressure profiles, triangularity has a clear, positive effect on the beta-limit, and for $\delta \geq 0.4$, the peaked pressure profiles give almost the same beta-limit as the broad profiles. For cross-sections of small triangularity, peaking of the pressure is clearly unfavourable and reasonably high betas can be reached only if the current profile has strong gradients in the central region, or if the central q is significantly above unity. This is needed for stability of Mercier and ballooning modes. In both types of optimisation, the beta-limit is rather weakly dependent on plasma current for safety factors at the plasma edge in the range of 2.2 to 5.

1. INTRODUCTION

For the design of the next generation of tokamaks, where the aim is to reach ignition and maintain thermonuclear burn, it is essential to find a configuration that allows operation with a beta of several percent. Beneficial effects of non-circularity can be seen from the scaling law [1]

$$g = \beta[\%] / I_N \leq g_{max} \approx 2.8 \ , \qquad (1a)$$

$$I_N = \mu_0 I / aB_0 \qquad (1b)$$

According to (1), an increase in the plasma current will increase the maximum beta, and it is clear, both from experiment and theory, that the required beta-values can only be achieved in plasmas of strongly non-circular cross-section, which allow significantly higher current than circular plasmas. (Note that the definition (1b) makes the normalised current I_N larger and, therefore, g smaller, by a factor $4\pi/10 \approx 1.257$ than the commonly used "engineering" definition I[MA]/a[m]B_0[T] for I_N. Also, note that, as a result of improved beta-optimisations, the maximum g in (1a) has been increased from the value 2.2 given originally in 1984 [1].) Recent studies [2,3] have shown that the linear dependence of the beta-limit on current (1) saturates at high current, when the safety factor at the edge is below 3. Thus, the scaling law (1) should be considered an upper limit, where equality cannot always be realised, and it is therefore important to know quantitatively how much the beta-limit is increased by shaping of the cross-section.

Besides the beta-limit, shaping modifies other operational limits for the tokamak. Such modifications may occur, not only in plasma current, but also in terms of the safety factor in the centre q_0 and at the edge q_s and in the shape of the current profile, coarsely quantified by the internal inductance ℓ_i.

A property of particular importance for ignition experiments is the ability to support the peaked pressure profiles expected to result from alpha particle heating. The importance of this point is underlined by the fact that the pressure profiles normally arrived at in beta-optimisations are flatter than those observed even in present-day, non-ignited experiments. This raises the question whether it may be impossible to reach the ideal-MHD beta-limit because it requires unrealistic profiles. Moreover, as the fusion output power is proportional to $\langle\beta^2\rangle$ (where $\beta=2p\mu_0/B_0^2$ and $\langle * \rangle$ denotes volume average), the pressure profiles that maximise the fusion power are more peaked than those that give the highest $\langle\beta\rangle$.

To investigate the effects of triangularity on the beta, and other, limits for NET/ITER-like tokamaks [4], we have carried out ideal-MHD stability studies, using the ERATO code [5]. The plasma boundary is specified as

$$r/a = A + \cos(\theta + \delta \sin\theta) \quad , \quad z/a = \kappa \sin\theta \quad . \qquad (2)$$

We have kept the elongation and aspect ratio fixed at $\kappa = 2$ and $A = 3.7$ (to keep continuity with previous work [6]), and studied four different triangularities: $\delta = 0.0$, 0.2, 0.4, and 0.6. The instabilities considered are the $n = 1$ free boundary kink and the $n=\infty$ ballooning (and Mercier) modes, and the criterion for kink stability was taken as $\gamma^2\tau_A{}^2 < 10^{-4}$.

One of our objectives was to investigate to what extent the beta-limit is sensitive to the equilibrium profiles, and whether, as a consequence, the usefulness of triangularity depends on the plasma profiles. Therefore, our optimisations have been made according to two different procedures. In the first group, the *current* profile is prescribed and the pressure profile is optimised. We impose two different current profiles, both of which are flat in the central region and decrease monotonically to zero at the edge. For such current profiles, maximum beta is obtained for broad pressure profiles, in particular, for low q_S and small triangularity. No gain results from a moderate triangularity; β_{max} remains constant at about 4.7 % for $\delta = 0.0$, 0.2 and 0.4, but the limit increases to about 5.9 % for high triangularity, $\delta = 0.6$. With broad current and pressure profiles, the main effect of triangularity is to increase the current limit, from $I_N \approx 2.3$ at $\delta = 0.0$ to $I_N \approx 3.0$ at $\delta = 0.6$. The current limit is reached at $q_S = 2$ for all triangularities considered here.

In the other set of optimisations, we specify a more *peaked pressure* profile and optimise the current profile. The peaked pressure profiles, when combined with standard current profiles, for which the central q is flat and near unity, tend to be unstable to localised, pressure driven modes (Mercier, ballooning, and intermediate-n) in the central region. These instabilities are more limiting for an ellipse than for a highly triangular plasma. It is well known [7] that Mercier stability is favoured by increasing one or more of (a) shear, (b) safety factor, and (c) triangularity. Therefore, we have applied two different modifications to the current profiles to improve on local stability in the centre. The first method consists of adding a central step to the current to increase the shear. The second consists of raising the central q. With either of these methods, the $n=1$ and $n = \infty$ modes give a beta-limit for peaked pressure profiles that is almost unchanged from that for broad profiles, if the cross-section is *sufficiently triangular*, $\delta \geq 0.4$. By contrast, in an *elliptical* cross-section, $\delta = 0.0$, the maximum beta decreases

significantly for the peaked profiles; from 4.7 % with a broad pressure profile to 3.9 % for a moderately peaked profile and 3.0 % for a strongly peaked profile. Furthermore, in an elliptical cross-section, rather non-standard current profiles are required to reach reasonably high beta with a peaked pressure profile. On the other hand, at high triangularity, $\delta = 0.6$, only slight modifications from standard current profiles are needed to confine high beta, even with a strongly peaked pressure profile.

We have made spot checks on the intermediate-n stability of the peaked pressure profiles. These checks show that the high-shear profiles optimised for $n = 1$ and $n = \infty$ are also stable for $n = 2$, 3, and 4. However, the profiles with a flat central current profile and raised q_0, optimised for $n = 1$ and $n = \infty$, tend to be unstable to intermediate-n (e.g., $n = 3$ and $n = 4$) modes. For peaked pressure profiles it appears that, unless sufficient shear is maintained in the central region, intermediate-n modes give a somewhat lower beta-limit than $n = 1$ and $n = \infty$.

2. PARAMETRISATION OF THE EQUILIBRIUM

The equilibria are computed with a version [8] of the EQLAUS code, which allows the specification of pressure gradient, $p' = dp/d\psi$ (where ψ is the poloidal flux) and surface averaged toroidal current density,

$$I' = \langle J_\phi \rangle = \frac{\int J_\phi \, dl / |\nabla\psi|}{\int dl / |\nabla\psi|} \quad , \tag{3}$$

as functions of ψ. The profiles for p' and I' are given as piecewise polynomials. With $\psi = 0$ on the magnetic axis and $\psi = \psi_S$ at the plasma surface, the current profile is parametrised according to

$$I'(\psi) = \begin{cases} \text{quadratic polynomial,} & 0 \le \psi < \psi_{I1} \ , \\ \text{cubic polynomial,} & \psi_{I1} \le \psi < \psi_{I2} \ , \\ \text{linear polynomial,} & \psi_{I2} \le \psi \le \psi_S \ . \end{cases} \tag{4}$$

The matching points ψ_{I1} and ψ_{I2} are free parameters, and the polynomials are chosen so that the resulting I' and its first derivative are everywhere continuous. For all equilibria, except those specially designated to investigate surface kink modes, we have used $I' = 0$

and $dI'/d\psi = 0$ at the plasma edge, $\psi_{I2} < \psi < \psi_S$ (in most cases, $\psi_{I2} = \psi_S$). Similarly, the pressure profile is given as a combination of polynomials,

$$p'(\psi) = \begin{cases} 0 \quad , & 0 \le \psi < \psi_{p1} \quad , \\ \text{cubic polynomial,} & \psi_{p1} \le \psi < \psi_{p2} \quad , \\ \text{quadratic polynomial,} & \psi_{p2} \le \psi \le \psi_S \quad , \end{cases} \qquad (5)$$

with p' and $dp'/d\psi$ everywhere continuous. The matching points ψ_{p1} and ψ_{p2} are independent from those for the current profile. We have restricted ourselves to profiles with $dp'/d\psi(\psi_{p2}) = 0$.

To construct current profiles with high central shear for the peaked pressure profiles, we have used an I' that is a superposition of two profiles of the form (4). The added contribution is in the form of a rounded step placed at the ψ-value where the pressure gradient starts to increase.

3. CENTRALLY FLAT CURRENT PROFILES, OPTIMISED PRESSURE PROFILES

This section presents results obtained by optimisation of the pressure profile for prescribed current profiles. Two different profiles have been used for the toroidal current: (a) a Shafranov, or "top-hat", profile, slightly rounded off for numerical reasons [with $\psi_{I2} = \psi_{I1} + 0.1\psi_S$, see Eq. (4)], and (b) a more rounded profile for which $\langle J_\phi \rangle$ is constant in the central region and goes to zero quadratically at the edge [as a cubic polynomial in ψ with zero slope both at the inner matching point $\psi = \psi_{I2}$ and at the plasma edge $\psi = \psi_{I2} = \psi_S$ in Eq. (4)]. The safety factor at the edge q_S varies from 2 to 6.5 and four values of triangularity have been considered: $\delta = 0.0$, 0.2, 0.4, and 0.6. In an initial study, we also varied the central q in the range $1.02 < q_0 < 1.12$. However, with the optimised, broad pressure profiles, the beta-limit is rather insensitive to q_0 and we give results for only one value, $q_0 = 1.07$. The pressure profile was optimised without any other constraint than ideal MHD stability, and we have tried to approximate, as closely as possible, the ballooning limit, starting from the *outside* of the plasma. In most cases described here, local pressure-driven modes are the limiting factor for beta, and in such cases the optimised pressure profile is close to the ballooning/Mercier limit over the whole cross-section.

3.1. Results

The beta-limits obtained after optimisation of the pressure profile for the broader current profile (b) are shown in Fig. 1. Figure (1a) shows β_{max} as a function of the normalised current, I_N, Fig. (1b) shows β_{max} as a function of safety factor at the edge, q_S, and (1c) shows the ratio $g = \beta_{max}/I_N$ vs I_N. (Note that q is the true geometrical safety factor. In strongly non-circular cases, q_S tends to depend more strongly on the plasma current than the $1/I_N$ dependence found for near-circular, low-beta plasmas. This is due to the formation of regions with weak poloidal field, which occur when I' is small and p' large near the edge, as is typical of the beta-optimised equilibria.)

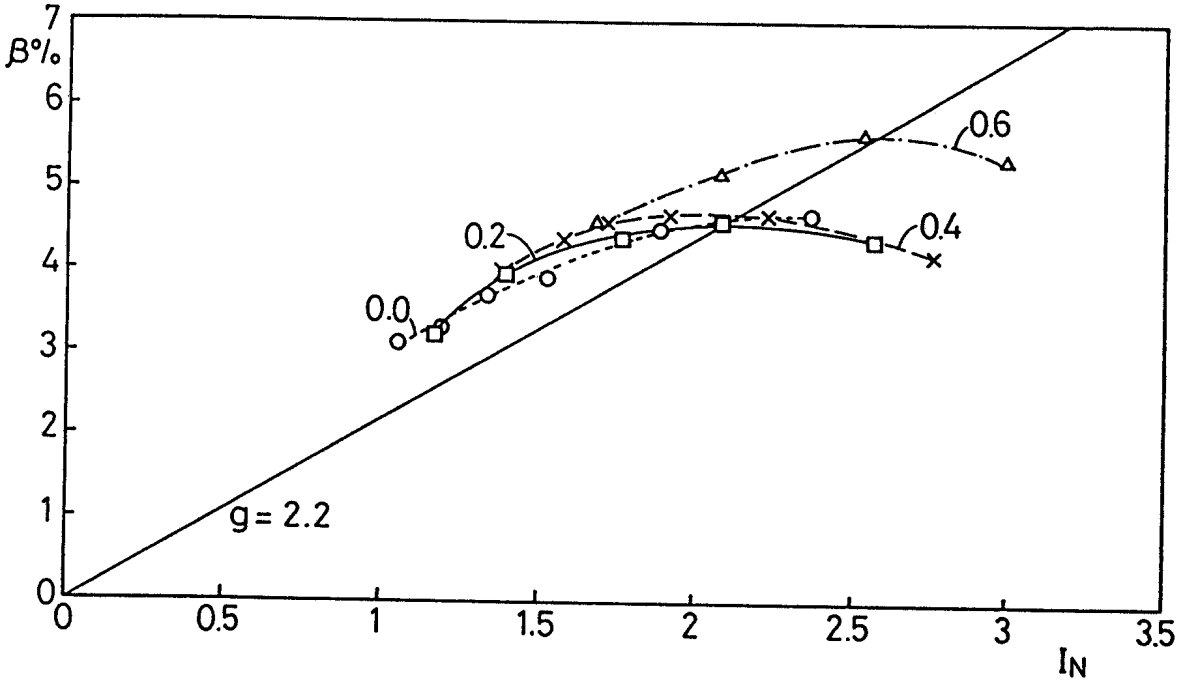

Figure 1(a). Optimised beta, β_{max}, vs normalised current, I_N for different triangularities δ: 0 0, 0.2, 0.4 and 0.6, aspect ratio A = 3.7 and the elongation κ=2. The profile for the averaged toroidal current is prescribed as flat in the central region, zero at the edge, and a cubic polynomial in between with zero derivative at the end points. The straight line shown is $g = \beta / I_N$ =2.2.

Figures 1a and 1b show that, for the broad profiles, the beta-limit is almost independent of triangularity for $0 \le \delta \le 0.4$, where $\beta_{max} \approx 4.6$ %. A certain gain results from increasing δ to 0.6, which gives $\beta_{max} \approx 5.6$ %. However, triangularity has a stronger effect on the maximum normalised current which increases from about 2.35 at δ = 0 to about 3 at $\delta = 0.6$. As a consequence, $g = \beta_{max}/I_N$ decreases with triangularity.

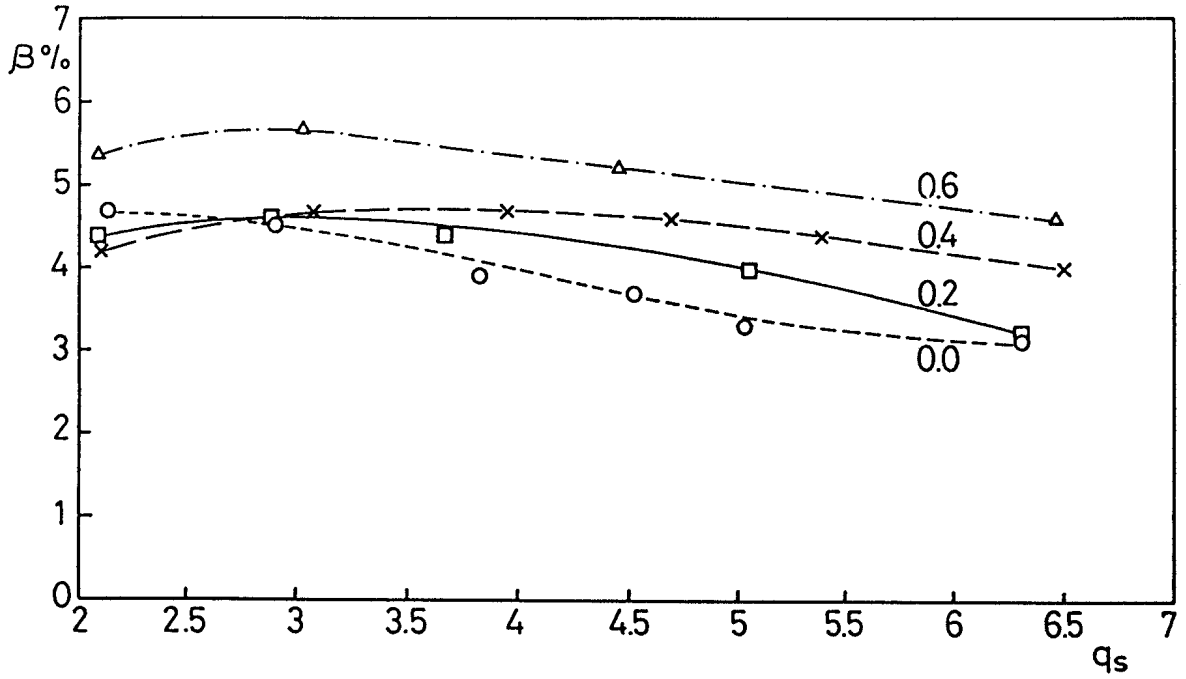

Figure 1(b). Optimised beta, β_{max} vs edge q for different triangularities δ: 0 0, 0.2, 0.4 and 0.6, aspect ratio A = 3.7 and the elongation κ=2.

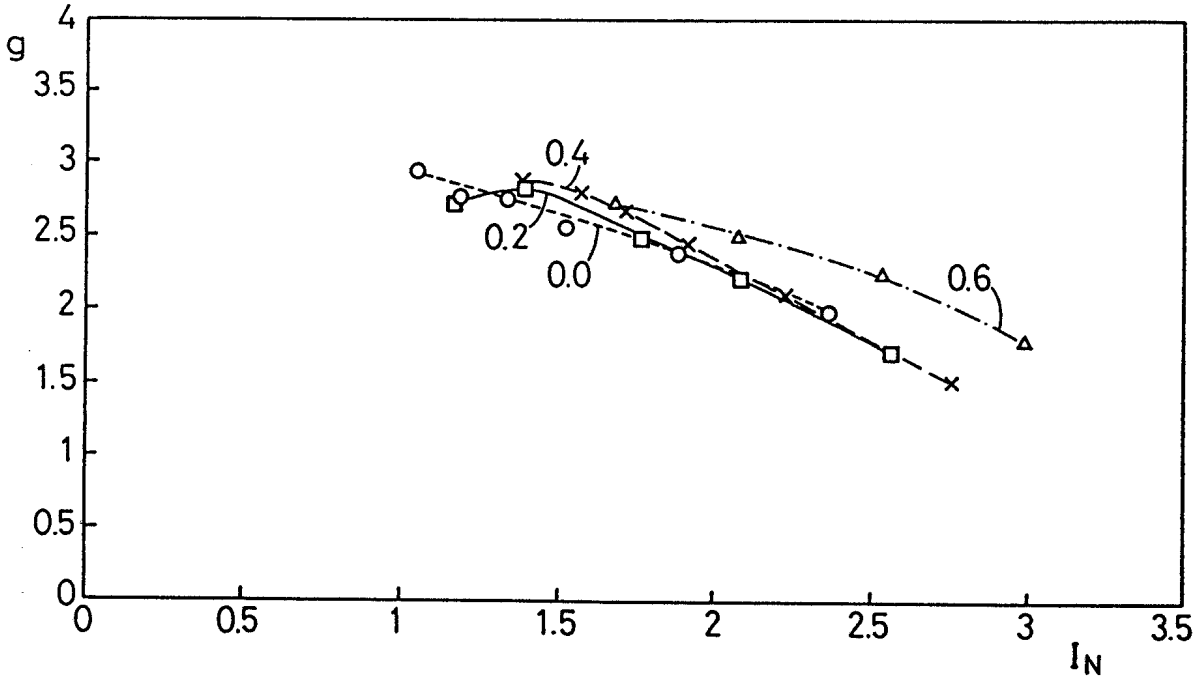

Figure 1(c). $g = \beta_{max} / I_N$ vs I_N for different triangularities δ: 0 0, 0.2, 0.4 and 0.6, aspect ratio A = 3.7 and the elongation κ=2.

Figure 1b shows that for fixed geometry, the beta-limit is only weakly dependent on the current when the safety factor is in the range $2.2 < q_s < 5$. This allows considerable freedom in operating space without significant reduction of the beta-limit. It is also clear

that an optimum value of I_N cannot be unambiguously determined from the present study. For example, small changes in q_0 lead to rather large changes in the optimum I_N.

In summary, high triangularity allows larger current and somewhat increases the beta-limit for the centrally flat current profile, while g decreases with increasing current. Interestingly enough, the line g = 2.2, originally proposed as the beta-limit in Ref. [1], gives rather a good fit for the highest beta-value obtained at each triangularity, although it does not correctly reproduce the variation of β_{max} with current for fixed geometry. Similar results have been obtained for circular equilibria [3]. With q_0 held fixed at 1.07, the beta-limit is usually set by ballooning/Mercier modes, except for large triangularity and high current $q_S < 3$, where the limit is set by the n = 1 kink mode.

3.2. Profiles

Figure 1b shows that β_{max} does not degrade significantly for $q_S < 3$. Such degradation as well as the so-called ravines in β_{max} for q_S just below integer values have been reported in other studies [2,9], in which $\langle J_\phi \rangle$ was not kept sufficiently small at the edge. We have investigated this issue in some detail by selecting current profiles with finite surface averaged toroidal current at the edge. Specifically two profiles have been examined, for which the ratio $\langle J_\phi \rangle(\psi_S) / \langle J_\phi \rangle(0)$ was 0.1 and 0.3, respectively [i.e., profile (4) with $\psi_{I2} = \psi_S$, $I'(\psi) = I'(0)$ for $0 \le \psi \le \psi_{I1}$ and $I'(\psi_S) / I'(0) = 0.1$ and 0.3, respectively.] For these profiles, instability of surface kink modes occurs for q_S below integers, in surprisingly good agreement with cylindrical large aspect ratio theory [10]. The growth-rates of the n = 1 kink mode for $\langle J_\phi \rangle(\psi_S) / \langle J_\phi \rangle(0) = 0.1$ and 0.3 and $\delta = 0.6$ are shown as functions of q_S in Fig. 2. The plasma beta is held fixed at 4.8 %, well below the stability limit for the pressure driven kink mode. Similar results were obtained at zero beta. Thus, surface kink modes are driven unstable by adverse distributions of current near the plasma surface and are almost independent of the pressure. It should be noted that in optimisations where the q-profile is specified rather than the current profile, the current density at the surface tends to increase with beta, and consequently, the surface kink mode may, in an artificial way, manifest itself as a reduction of the beta-limit. It is, however, clear that at low q_S, a highly triangular plasma is more susceptible to surface kink modes than an elliptical or circular one. The reason for this is the change in the current profile; triangularity contributes to the shear, so that for fixed q_0 and q_S, triangularity forces the current distribution to be flatter and more current to flow near the plasma edge. Our study shows that only moderate peaking of the current is required for kink stability below $q_S = 3$. Thus, operation with q_S between 2 and 3 should be possible, even at high triangularity $\delta = 0.6$. However, we find the highest beta-limit for

q_S above 3, and consequently, operation with $q_S < 3$ does not appear to be of strong interest for reaching high beta.

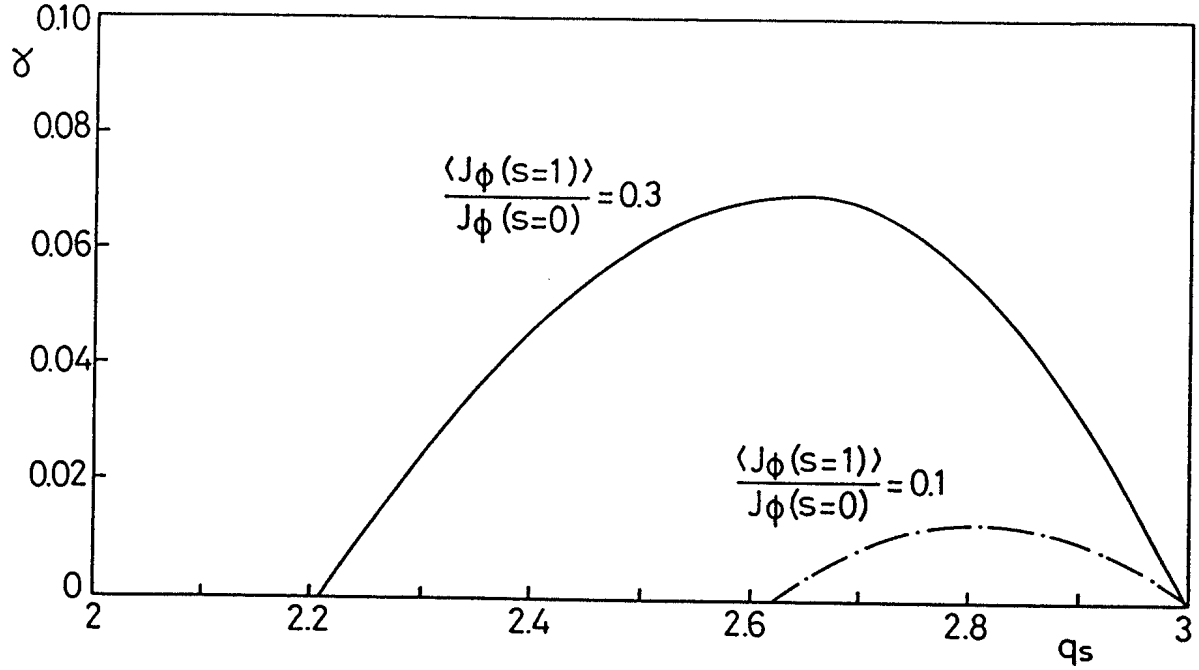

Figure 2. Growth-rate of surface kink mode as a function of q_S for cases where the surface averaged toroidal current density at the plasma edge is 10 % and 30 % of the central current density. In both cases, A = 3.7, $\kappa = 2$ and $\delta = 0.6$.

Figure 3 shows the equilibrium profiles of q and $q' = dq/d\psi$ versus $s=(\psi/\psi_S)^{1/2}$, together with the surface averaged toroidal current $I' = \langle J_\phi \rangle$ and optimised pressure p, versus major radius r in the mid-plane. The broader profile (b) was used for I' and the parameters are: in (3a) $\delta = 0.6$, $q_S = 4.45$ and in (3b) $\delta = 0$ and $q_S = 5.05$. Note that the optimised pressure profiles are rather broad, but that the triangular case $\delta = 0.6$ can confine some pressure gradients in the central region where I' = constant. For the elliptical equilibrium, p' goes rather abruptly to zero at a certain radius. This is required for the stability of Mercier and ballooning modes in the central low-shear region. Similar conditions prevail also for $\delta = 0.2$ and 0.4, and only for high triangularity $\delta = 0.6$ can significant pressure gradients be confined in the central region of flat current. This appears to be the reason why the $\delta = 0.6$ case gives a somewhat higher beta-limit than the lower triangularities. The ability of the $\delta = 0.6$ case to support larger pressure gradients in the central region is due both to the increased shear created by triangularity and to shaping of the magnetic surfaces, which makes the field-lines travel a long distance (i.e., the poloidal field is weak) in the regions where the curvature favourable. Nevertheless, for centrally flat current distributions, the pressure profiles optimised for volume average beta are rather broad. The effect of triangularity on the current profile is

clearly seen in Fig. 3: at fixed q_0 and q_s, the triangular case has a much broader current distribution.

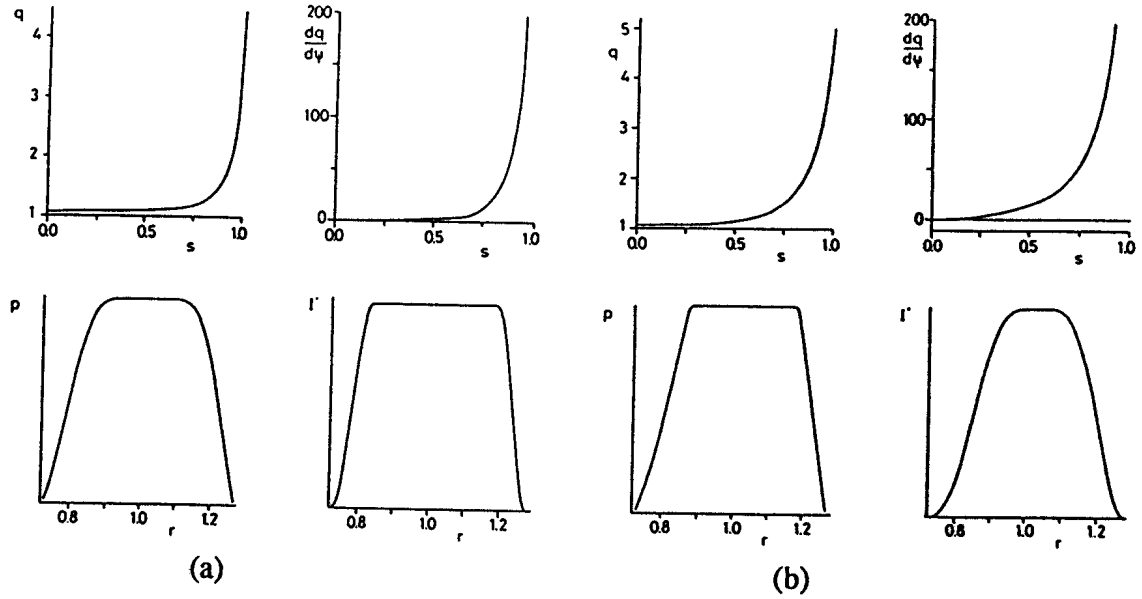

Figure 3. Profiles of q and q' = dq/dψ, vs s = $(\psi/\psi_s)^{1/2}$ together with surface averaged toroidal current I' and optimised pressure profile, vs major radius r in the mid-plane for the rounded current profile. In (a) $\delta = 0.6$ and $q_s = 4.44$, $\beta = 5.1$ %, $\beta^* = 6.1$ %, $\beta_0 = 10.0$ % and $\ell_i = 0.70$. In (b) $\delta = 0$ and $q_s = 5.05$, $\beta = 3.3$ %, $\beta^* = 3.9$ %, $\beta_0 = 6.1$ % and $\ell_i = 0.99$.

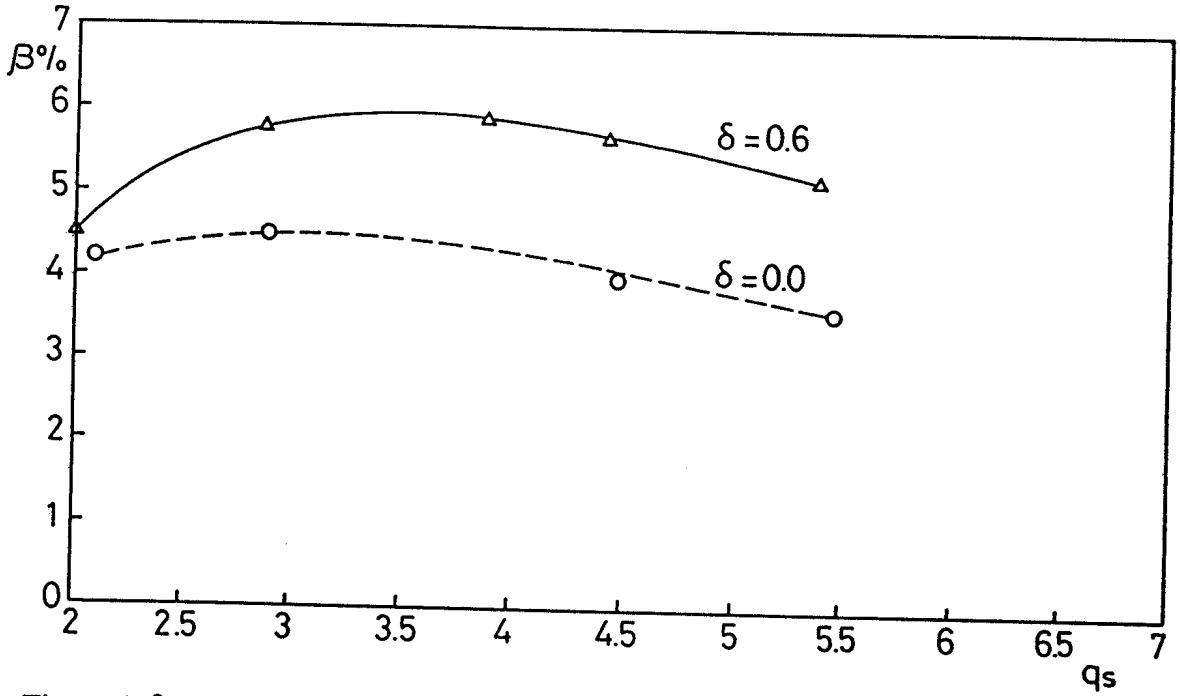

Figure 4. β_{max} as a function of q_s for Shafranov (top-hat) current profile for $\delta = 0$ and $\delta = 0.6$. Other parameters are identical to those in Fig. 1.

Figure 4 shows β_{max} vs. q_s for the Shafranov current profile. Comparison with Fig. 1b for the broader profile shows that the Shafranov profile gives a slightly higher beta-limit at high q_s, but the difference is very small. Thus, it appears that, for current profiles that are flat in the centre and where $<J_\phi>$ decreases monotonically to zero at the edge, the details of the current profile do not have a strong effect on the maximum achievable beta.

4. PEAKED PRESSURE PROFILES

Pressure profiles observed in most tokamaks are more peaked than those found to give the highest beta in ideal-MHD stability studies. Thus, the question arises whether it may not be possible to reach the theoretical beta-limit because it requires unrealistic profiles. This issue could become severe for an ignited tokamak, where alpha particle heating is expected to produce strongly peaked profiles. Another consideration is that the fusion power is not a function of the volume average beta, but is more accurately proportional to $\beta^{*2} = <\beta^2>$. To provide a basis for a more realistic assessment of the effects of triangularity, we have carried out optimisations of the current profile with prescribed, *peaked* pressure profiles. Two such pressure profiles are considered here; one "moderately peaked" where p = constant for $|r - R| < 0.4a$ and $dp/dr \approx$ constant for $|r-R| > 0.4a$, and one "strongly peaked" where $dp/dr \approx$ constant for $|r-R| > 0.1a$. (r is the major radius in the mid-plane z=0, and R is the major radius of the magnetic axis.)

Before giving results, we note that the ratio β^*/β is not very large, even for equilibria with strongly peaked pressure. For a circular equilibrium at large aspect ratio, with dp/dr = constant from the centre to the edge, $\beta^*/\beta = (1.5)^{1/2} \approx 1.22$, while the ratio of central to average beta is of course larger, $\beta_0/\beta = 3$. Needless to say, a factor $(\beta^*/\beta)^2$ between 1 and 1.5 in the power production can play a decisive role under marginal conditions.

4.1. Moderately peaked pressure

The beta-limit for the moderately peaked pressure profile, after optimisation of the current profile, is shown in Fig. 5. Fig. (5a) shows $\beta_{max}(I_N)$, (5b) $\beta_{max}(q_s)$ and (5c) $g(I_N)$ for the extreme values of triangularity, $\delta = 0.0$ and $\delta = 0.6$. For these equilibria, Mercier stability in the central region was ensured by introducing a step in the current density at the point where the pressure gradient becomes large, so as to increase

the shear. For the elliptical case, we have also made $dI'/d\psi(\psi_{I1})$ negative [see Eq. (4)] to increase the shear in the central region.

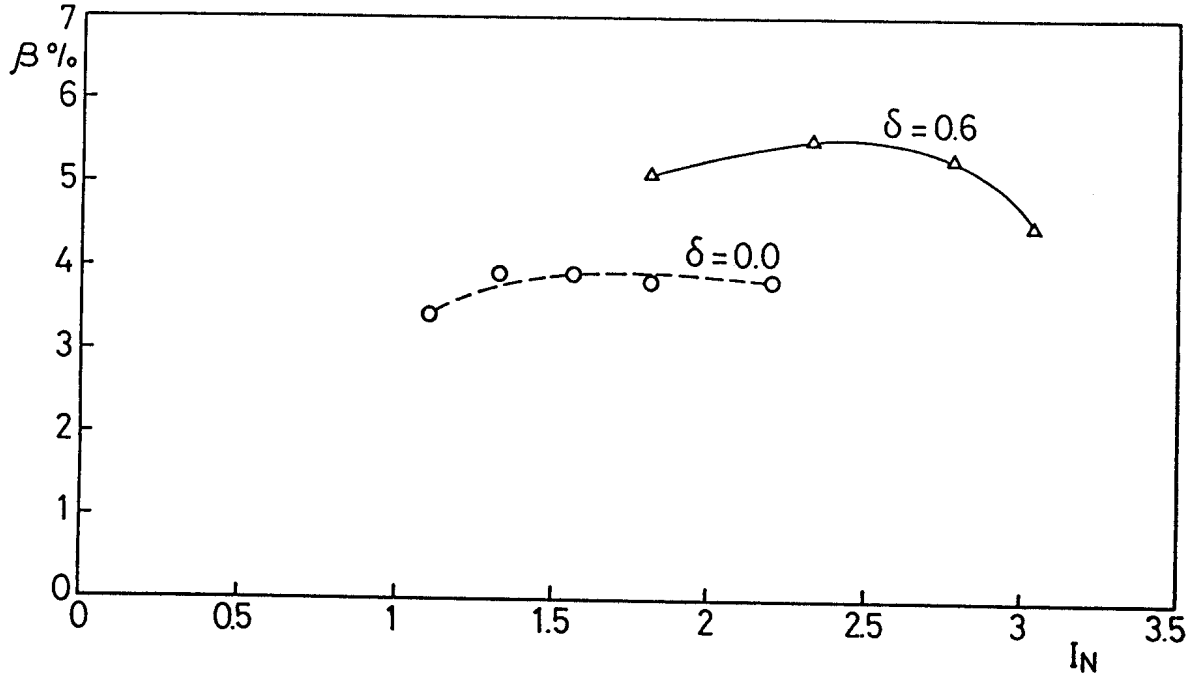

Figure 5(a). Optimised beta, β_{max}, vs normalised current, I_N. The pressure profile is prescribed as moderately peaked and the current profile has been optimised, using a central step for two triangularities δ: 0.0 and 0.6.

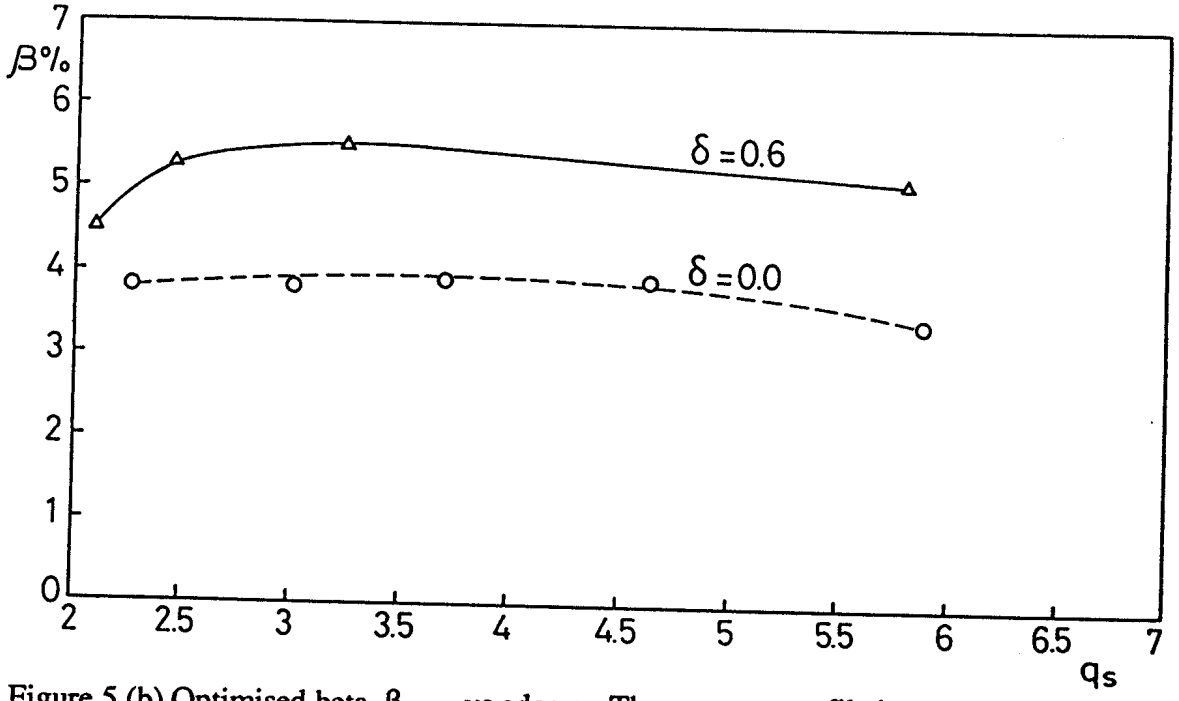

Figure 5.(b) Optimised beta, β_{max} vs edge q. The pressure profile is prescribed as moderately peaked and the current profile has been optimised, using a central step for two triangularities δ: 0.0 and 0.6.

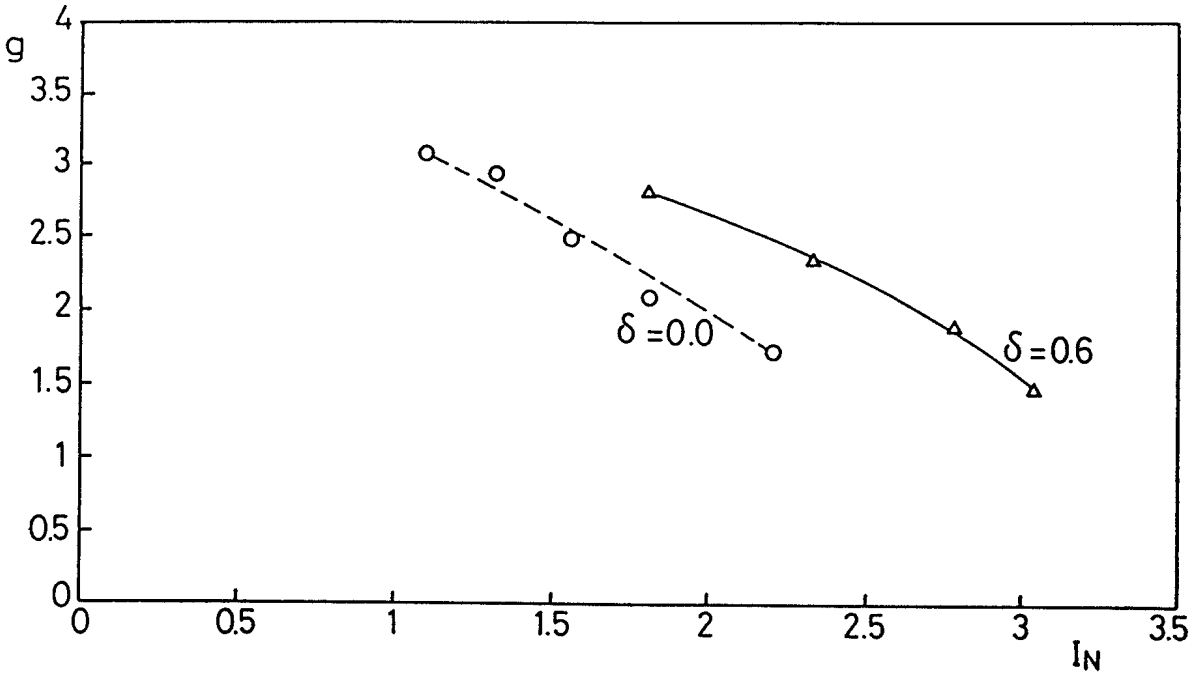

Figure 5(c). $g = \beta_{max} / I_N$ vs I_N. The pressure profile is prescribed as moderately peaked and the current profile has been optimised, using a central step for two triangularities δ: 0.0 and 0.6.

Comparison with Fig. 1 shows that no major reduction in the beta-limit results from constraining the pressure to the moderately peaked profile. In particular, we find no change from the broad profiles for $q_S > 4$, independent of the triangularity. At higher current, $q_S < 4$, β_{max} is somewhat smaller for the moderately peaked profile than for the broad profile. The decrease is larger for the ellipse. For example, at $q_S \approx 2.5$, β_{max} falls from about 4.5 % to 3.7 % for $\delta = 0.0$, while at high triangularity, the drop is insignificant, from 5.6 % to 5.5 %. The maximal values of β^* and β_0 that we have obtained for the moderately peaked pressure profile are $\beta^* = 6.5$ %, $\beta_0 = 11.7$ % at $\delta = 0.6$ and $\beta^* = 4.8$ %, $\beta_0 = 8.7$ % at $\delta = 0.0$.

Figure 6 shows the equilibrium profiles of q, $q' = dq/d\psi$, I' and p for the optimised current profiles in a highly triangular cross-section: (6a) for low q_S and (6b) for high q_S. At low q_S, the optimal current profile (6a) is flat in the central region and belongs to the class of profiles imposed in Sec. 3. It can be seen in Fig. (6a) that the increase in pressure gradient at $s \approx 0.4$ increases q', and this rather weak shear, in combination with the favourable shaping effect of triangularity, is sufficient for local stability. In the high-q case (6b) it was necessary to add a step of about 10 % to the current profile in the inner region to stabilise the Mercier and ballooning modes.

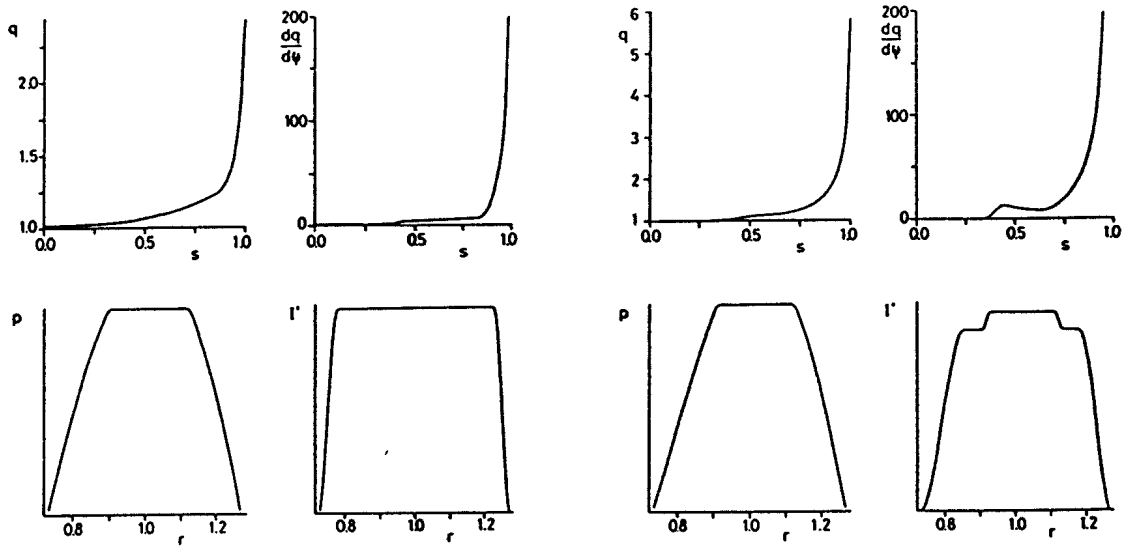

(a) (b)

Figure 6. Optimised profiles of q and q' = dq/dψ, vs s = $(\psi/\psi_s)^{1/2}$ together with surface averaged toroidal current I' and pressure profile, vs major radius r in the mid-plane for the moderately peaked pressure profile and high triangularity δ = 0.6. In (a) q_s = 2.42, β = 5.5 %, β* = 6.4 %, β_0 = 11.9 %, and ℓ_i = 0.52 and in (b) q_s = 5.81, β = 5.1 % , β* = 6.3 %, β_0 = 11.8 %, and ℓ_i = 0.76.

Figure 7 shows the corresponding profiles for the ellipse, where the optimal current step is larger, about 20 %, both at high and low q_s. Thus, an elliptical plasma needs stronger modifications in the current profile to accommodate the peaked pressure profile than does a highly triangular one. In addition, the drop in β_{max} relative to the broad profile is more pronounced for the ellipse. This is to be expected, as triangularity has a strongly stabilising effect on the Mercier modes [7].

Some comments on the optimisation procedure are in order. Although the pressure profile has been fixed, more freedom has now been introduced in the current profile, where both the magnitude and width of the step can be varied. The extra degrees of freedom have allowed us, in most cases, to optimise by a trade-off between kink and Mercier/ballooning stability, so that both become unstable at the same value of beta. Increasing the height of the step improves the local stability in the centre, but degrades kink stability if q_0 is kept fixed. The results quoted in Figs. 5 - 7 were obtained for a fixed central q of q_0 = 1.02.

It should also be remarked that, although ballooning modes are necessarily unstable whenever the Mercier criterion is violated, there are cases where the Mercier criterion predicts instability, and we do not observe ballooning instability numerically. This happens in the central region of low shear, where the unstable ballooning modes are

close to interchange modes. These interchange-like ballooning modes are strongly localised radially and broad in the generalised poloidal angle χ. The χ-interval required to capture such modes can be of the order of a hundred poloidal turns, which is much larger than the $15 \times 2\pi$ that we routinely use. However, these modes are readily found by the Mercier criterion and are very distinct from the strongly ballooning modes that occur where the shear is large. In the present study, we consider a profile locally stable when, and only when, the Mercier criterion for stability is satisfied and no unstable ballooning mode occurs over 15 turns in χ. For the peaked pressure profiles (in particular, the strongly peaked profiles, see Sec. 4.2), the most limiting of the local modes is, in fact, interchange in the central low-shear region.

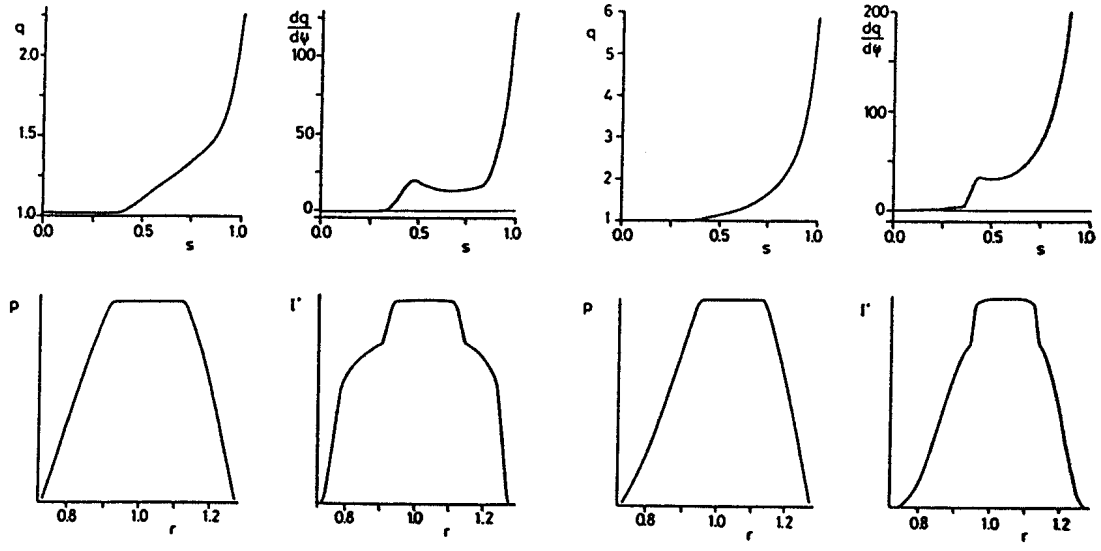

Figure 7. Optimised profiles of q and q' = dq/dψ, vs s = $(\psi/\psi_s)^{1/2}$ together with surface averaged toroidal current I' and pressure profile, vs major radius r in the mid-plane for the moderately peaked pressure profile and zero triangularity. In (a) q_s = 2.26, β = 3.9 %, β^* = 4.6 %, β_0 = 7.6 %, and ℓ_i = 0.64 and in (b) q_s = 5.88, β = 3.4 %, β^* = 4.3 %, β_0 = 8.7 %, and ℓ_i = 1.01.

4.2. Strongly peaked pressure

The tendencies found for the moderately peaked pressure profile become more pronounced in the optimisations with a *strongly peaked pressure profile*. The beta-limit remains about equal to that for the broad profiles when the triangularity is sufficient, $\delta \geq 0.4$, but falls significantly for lower triangularities. More pronounced modifications

of the current profile are, of course, required in this case than for the moderately peaked pressure profile.

To test the sensitivity of the results to the choice of current profile, we have applied two different classes of current profiles, corresponding to different strategies for improving Mercier stability in the central region. The first class is similar to that in Sec. 4.1. These profiles have a rounded step in the current density to increase the shear near the centre and a negative derivative of I' at ψ_{I1}. The second class has a reduced central current density or, equivalently, an increased q_0. For both these types of current profiles, the cases with $\delta \geq 0.4$ give beta-limits for $n = 1$ and $n = \infty$ stability close to those for the broad pressure profile. For small triangularity, $\delta = 0.2$, and even more so for $\delta = 0.0$, the beta-limit for strongly peaked pressure is substantially lower than for the broad profiles.

Figure 8 shows the beta-limits for strongly peaked pressure, obtained with the high-shear current profile and q_0 held fixed at 1.02.

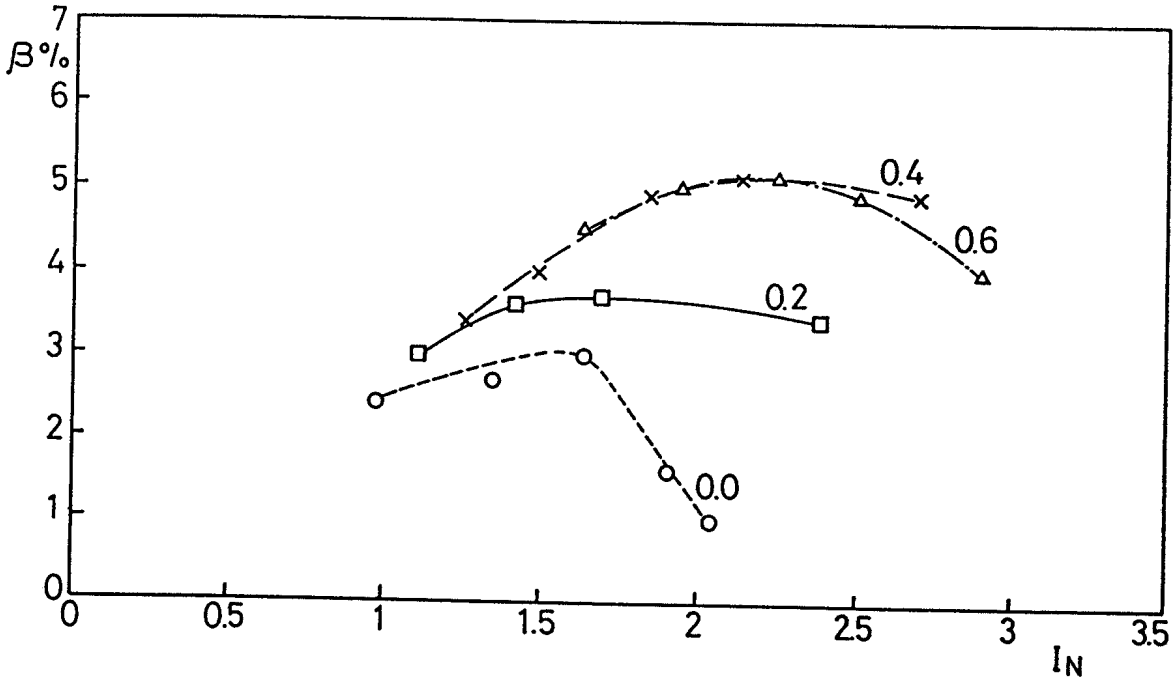

Figure 8(a). Optimised beta, β_{max}, vs normalised current, I_N for triangularities $\delta =$ 0.0, 0.2, 0.4, and 0.6. The pressure profile is prescribed as strongly peaked and the current profile has been optimised, using a central step.

For high triangularity, there are relatively minor differences from the results obtained for the broad profiles. Notably, β_{max} for $\delta = 0.6$ drops slightly from 5.6 % to 5.1 %, while for $\delta = 0.4$, the peaked pressure plus optimised current profile even improves the maximum beta from about 4.6% to 5.2 %. Figure 8a shows that beta as a function of

current is almost the same for $\delta = 0.4$ and $\delta = 0.6$. The two curves in Fig. 8a show broad maxima of $\beta_{max} \approx 5.1$ % at $I_N \approx 2.2$, where q_s is about 3.1 and 3.7, respectively.

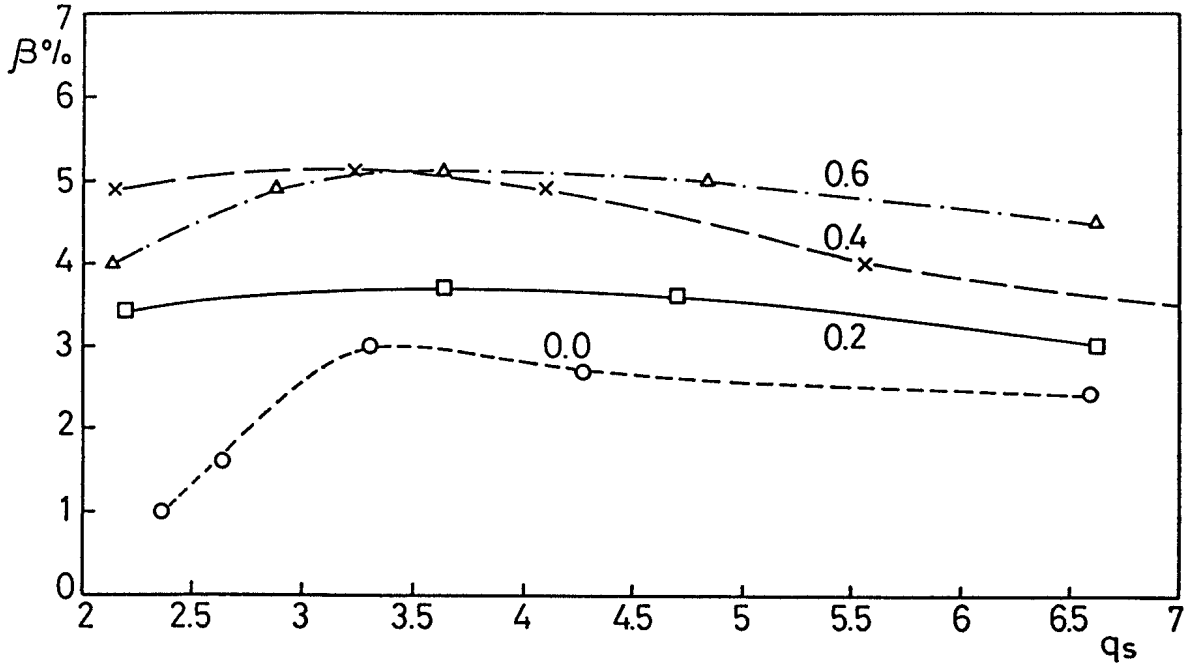

Figure 8(b). Optimised beta, β_{max} vs edge q for triangularities $\delta =$ 0.0, 0.2, 0.4, and 0.6. The pressure profile is prescribed as strongly peaked and the current profile has been optimised, using a central step .

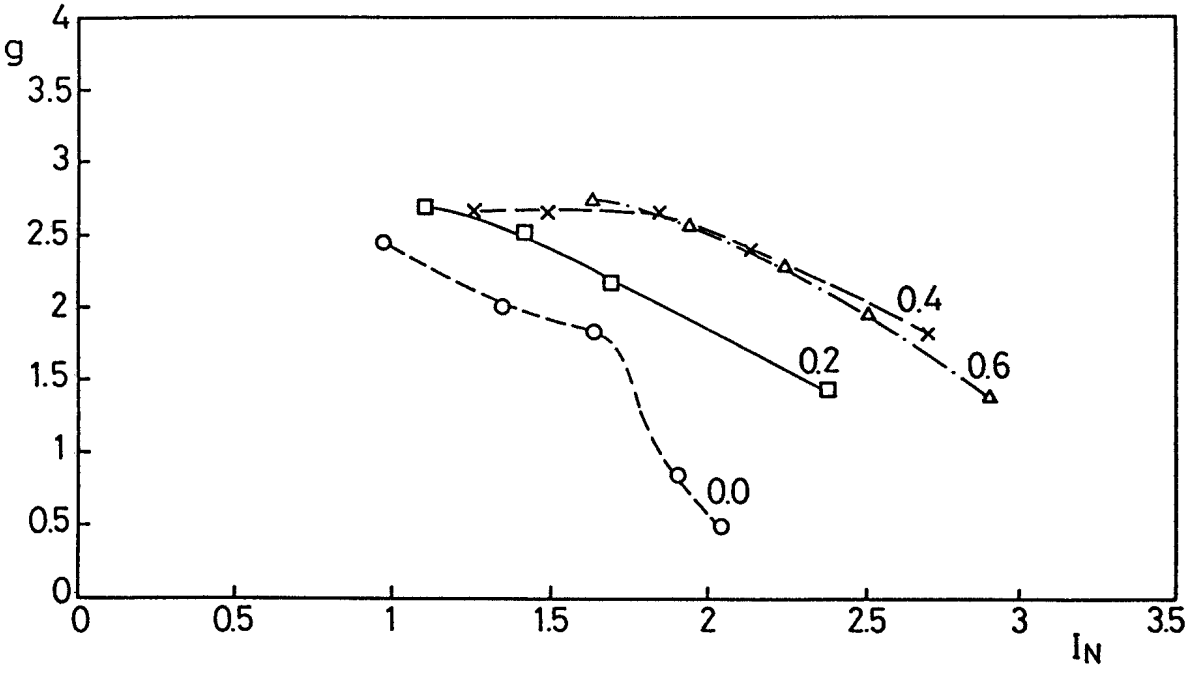

Figure 8(c). $g = \beta_{max} / I_N$ vs I_N for triangularities $\delta =$ 0.0, 0.2, 0.4, and 0.6. The pressure profile is prescribed as strongly peaked and the current profile has been optimised, using a central step .

(As remarked in Sec. 3, the optimum q_s is sensitive to details, such as, e.g., the value of q_0.) For $\delta = 0.6$, we find $\beta_{max} \approx 5.1$ %, with $\beta^* \approx 6.4$ % and a central beta of $\beta_0 \approx 14.5$ %, and $\delta = 0.4$ gives almost identical values.

For lower triangularity $\delta = 0.2$, and in particular, for the ellipse, the beta-limit degrades for the peaked pressure profile. For instance, $\delta = 0.0$ gives $\beta_{max} \approx 3.0$ % with $\beta^* \approx 3.7$ %, which is significantly lower than for the broad and moderately peaked cases. In fact, even the central beta of 8.3 % is lower than the 8.7 % reached with the moderately peaked profile. Thus, it is clear that the ellipse cannot confine a peaked pressure well.

To indicate what current profiles are required to give sufficient central shear for a strongly peaked pressure profile and $q_0 = 1.02$, we show in Fig. 9 optimised equilibria with (a) $\delta = 0.6$, $q_s = 3.65$ and (b) $\delta = 0.0$, $q_s = 3.31$. The height of the step is about 10 % for the triangular equilibrium and 30 % for the ellipse. As expected, triangularity reduces the amount of shear needed for Mercier stability in the centre. The optimal height of the step increases with q_s.

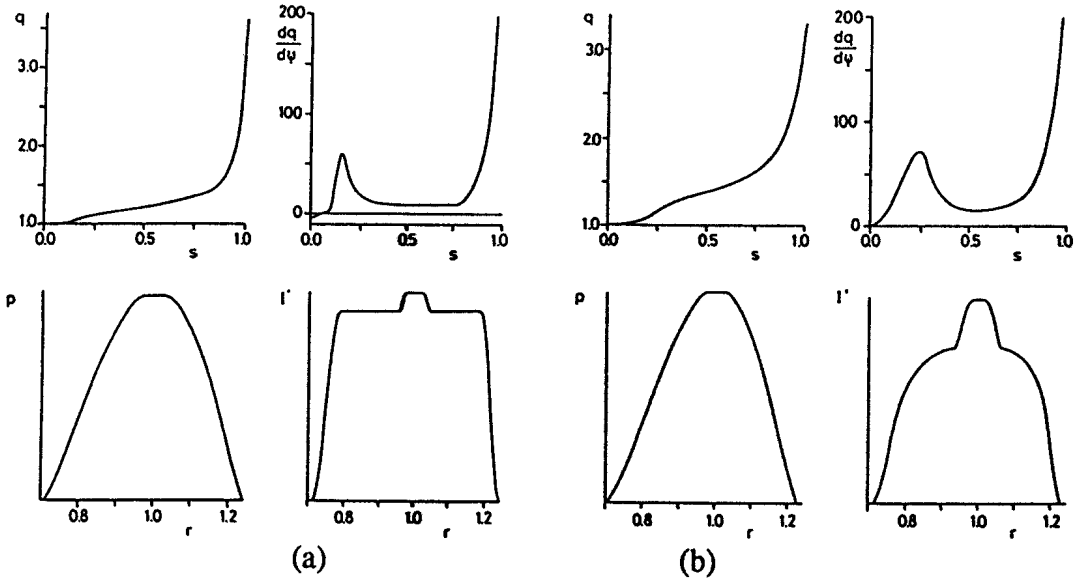

Figure 9. Equilibria with strongly peaked pressure profile and optimised, high-shear current profile. In (a) $\delta = 0.6$, $q_s = 3.65$, $\beta = 5.2$ %, $\beta^* = 6.5$ %, $\beta_0 = 14.7$ %, and $l_i = 0.58$. In (b) $\delta = 0.0$, $q_s = 3.31$, $\beta = 2.9$ %, $\beta^* = 3.6$ %, $\beta_0 = 8.0$ %, and $l_i = 0.72$.

Stability to n =1 and n = ∞ modes can also be achieved, even for a centrally flat current distribution, by increasing q_0. The resulting beta-limits are shown in Fig. 10. Here, the current profile is the broad profile of Sec. 3, and q_0 has been optimised. The step size for the optimisation of q_0 was 0.05 and we used the numerical values q_0 =

1.02, 1.07, etc. In most of these optimised equilibria, q_0 is clearly above unity, corresponding to sawtooth-free operation. The highest beta is reached for $\delta = 0.4$, where $\beta = 5.4$ %, $\beta^* = 6.8$ %, and $\beta_0 = 15.0$ %. Similar to the case of high-shear current profiles, the beta-limit at $\delta = 0.4$ for peaked pressure with optimised q_0 is higher than for the broad pressure profile in Sec. 3.

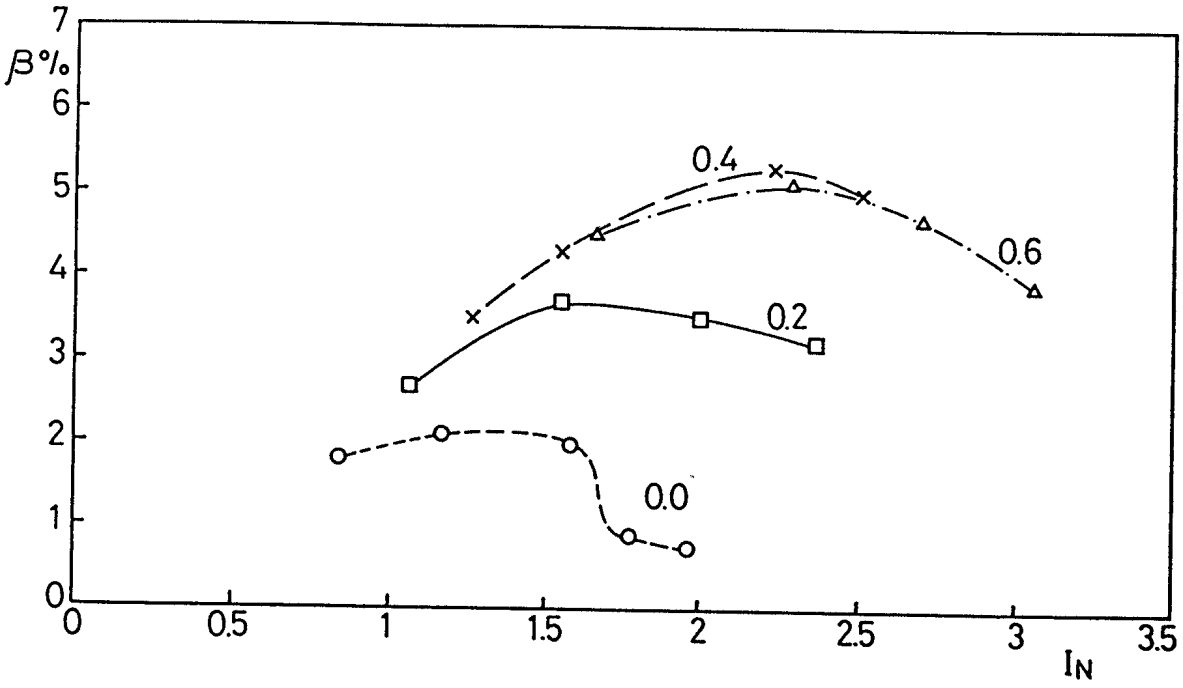

Figure 10(a). Optimised beta, β_{max}, for n = 1 and n = ∞ stability, vs normalised current, I_N for triangularities $\delta =$ 0.0, 0.2, 0.4, and 0.6. The pressure profile is prescribed as strongly peaked and the current profile has been optimised by raising q_0. Note that these equilibria tend to be unstable to intermediate-n modes.

The similarity of the results for raised q_0 (Fig. 10) with those obtained for the high-shear current profile (Fig. 8) is striking. Minor differences may be noted, for example, a lower beta-limit for low triangularity and high current for the equilibria with raised q_0. This is due to difficulty with kink stability at small q_s/q_0. For the ellipse, the drop for $q_s < 3$ is pronounced and has the character of a ravine [2,9]. For this case, the central q is 1.52, so that $q_s/q_0 < 2$ and kink stability is strongly reduced. We find that the optimum value of q_0 decreases with increasing triangularity and increases slowly with q_s. For the optimised equilibria in Fig. 10, q_0 goes from 1.02 at $q_s = 2.0$ to 1.12 at $q_s = 6.5$ for $\delta = 0.6$, from 1.12 to 1.27 for $\delta = 0.4$, from 1.27 to 1.37 for $\delta = 0.2$, and from 1.52 to 1.57 for $\delta = 0.0$.

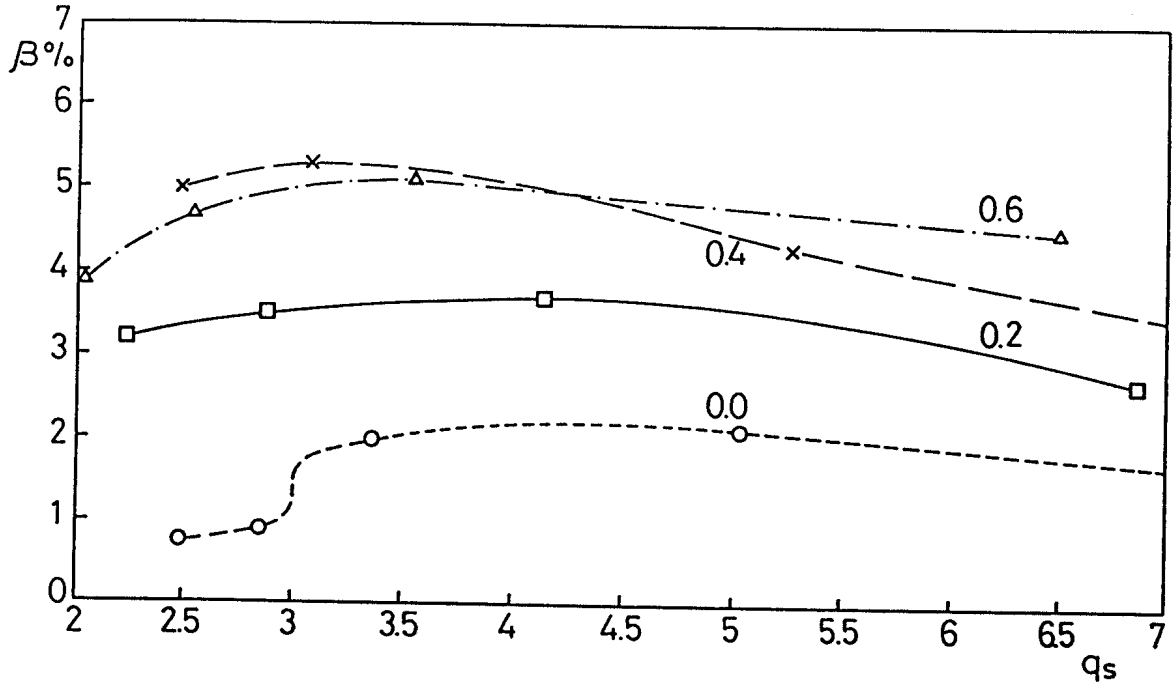

Figure 10(b). Optimised beta, β_{max} vs edge q for triangularities $\delta =$ 0.0, 0.2, 0.4, and 0.6. The pressure profile is prescribed as strongly peaked and the current profile has been optimised by raising q_0 .

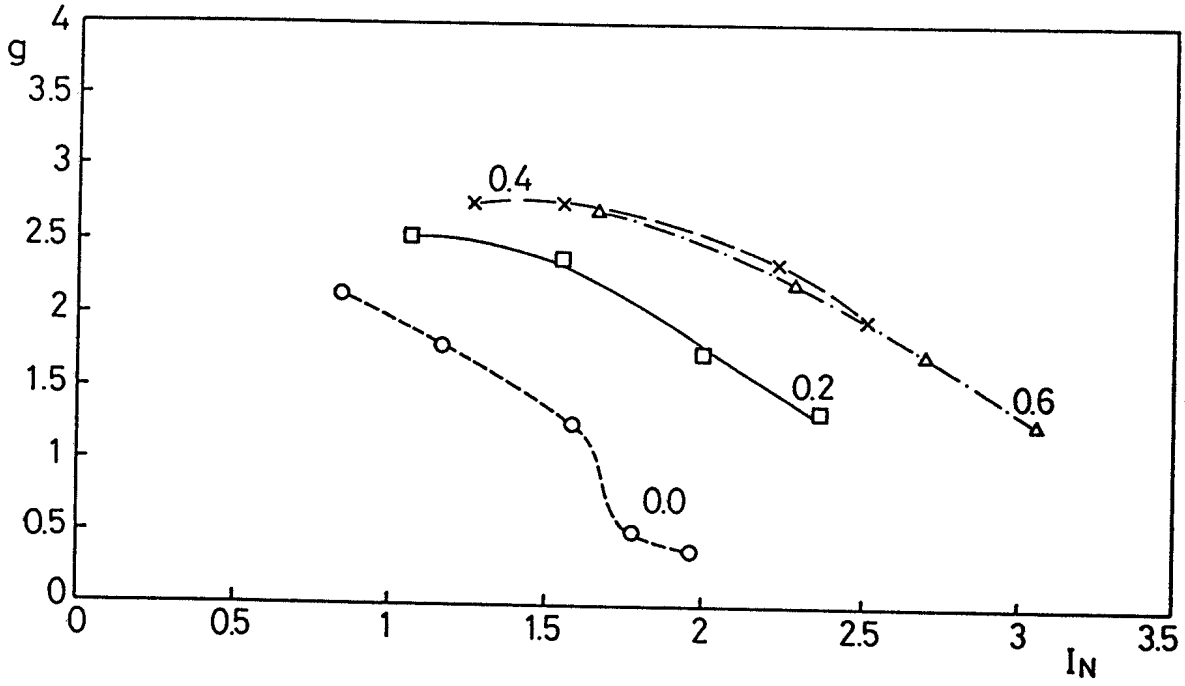

Figure 10(c). $g = \beta_{max} / I_N$ vs I_N for triangularities $\delta =$ 0.0, 0.2, 0.4, and 0.6. The pressure profile is prescribed as strongly peaked and the current profile has been optimised by raising q_0 .

The important difference between the high-shear equilibria and those with a raised q_0 lies in the stability to intermediate-n modes. Manickam et al [11] found that for equilibria with large pressure gradients in a central region of low shear, intermediate-n, so-called "infernal", modes can be unstable even though both the n = 1 and ballooning modes are stable. We have made spot checks of the n = 2, 3, and 4 stability of the two sets of equilibria with peaked pressure profile, optimised for n =1 and n = ∞ stability. We find that, whereas the the high-shear profiles (Figs. 8 and 9) are generally stable, the low-shear profiles with a raised q_0 tend to be unstable to the infernal modes. However, it appears that the beta-limit set by infernal modes for these profiles is only slightly lower than the n = 1, n = ∞ limit.

It is clear that shear in the central region is very helpful to achieve complete ideal-MHD stability at high beta with a strongly peaked pressure. As noted before, the necessary central current gradients decrease with increasing triangularity. The effects of central shear, q_0, and flux surface shaping on the stability of infernal modes clearly merit further study in the case of peaked pressure profiles.

Two effects of triangularity become evident in the optimisation with peaked pressure profiles. One effect, which is clearly advantageous, is the *shaping* of the flux surfaces. With positive δ and $\kappa > 1$, the two sharp tips of the triangular flux surfaces, where the field lines spend a large part of the time, lie in regions of favourable curvature, which improves stability to pressure driven modes. It is clear from Figs. 6-8 that the triangular case $\delta = 0.6$ can confine stronger pressure gradients in the central region with less shear than the elliptical cross-section.

A second effect of triangularity is to increase the *shear* for a fixed current profile. This occurs because the triangularity of the flux surfaces, which has the effect of raising q, increases with radius (approximately linearly). This effect on the shear is enhanced by finite pressure gradients. On the other hand, the *ellipticity* of the flux surfaces remains approximately constant with radius and therefore does not contribute to the shear in the same way. The difference between the current profiles for $\delta = 0.0$ and $\delta = 0.6$ in Figs. 6-8 can also be seen from the lower internal inductance ℓ_i at the same q_S for the triangular cross-section. It is, however, not obvious that the effect of large triangularity on the relation between the current and q-profiles is a practical advantage. The current profiles used here for $\delta = 0.6$ are flat over most of the cross-section, and the fall-off of the toroidal current density starts where q is already significantly above unity. This is the case, in particular, for equilibria with low q_S. Such profiles cannot be maintained in ohmic equilibrium, and will require substantial current drive.

5. SUMMARY AND CONCLUSION

For broad pressure profiles, the influence of triangularity on the beta-limit is weak for triangularities δ in the range 0 to 0.4 (where $\beta_{max} \approx 4.6$ %), but some positive effect is seen when δ is increased to 0.6 (giving $\beta_{max} \approx 5.6$ %). The dependence on plasma current is weak for $2.2 < q_S < 5$. For current profiles where $\langle J_\phi \rangle$ goes to zero smoothly at the plasma edge, no pronounced deterioration of the beta limit occurs for $2 < q_S < 3$, and no ravines occur for q_S just below integers.

Optimisations with prescribed, *peaked* pressure profiles show clearly advantageous effects of triangularity, and for $\delta \geq 0.4$, high beta can still be confined by an optimised current profile. Stability to $n = 1$ and $n = \infty$ modes with a peaked pressure profile can be achieved, either by means of central current gradients giving high shear near the centre, or by raising q_0. Intermediate-n modes slightly decrease the beta-limit for the low-shear profiles with a raised q_0, but do not appear to be a limiting factor for equilibria with strong central shear. For the strongly peaked pressure profile, we find a maximum beta of about 5.1 % both for $\delta = 0.4$ and $\delta = 0.6$, with $\beta^* = 6.4$ % and a central beta $\beta_0 = 14.5$ %. For the ellipse, these values are considerably lower, $\beta_{max} = 3.0$ %, $\beta^* = 3.7$ % and $\beta_0 = 8.3$ %. In addition, the ellipse requires pronounced central current gradients to confine reasonably high beta with a peaked pressure profile. In the absence of such current gradients, the beta-limit for an elliptical plasma decreases drastically when a peaked pressure profile is imposed. By contrast, highly triangular plasmas with $\delta \geq 0.4$ only need slight modifications of the central current profile to support the peaked pressure profile.

We note that the influence of the equilibrium profiles discussed here resolve conflicting results of previous investigations [2,6,12] concerning the effect of triangularity. Todd et al [12] used a strongly peaked pressure profile, where $dp/d\psi$ is maximum in the centre. This study indicated a clearly favourable effect of triangularity. Yasseen et al [6] used a top-hat current profile and optimised the pressure profile. This procedure gave rise to a broad pressure profile, in agreement with the present study, and essentially no difference in the beta-limit between $\delta = 0.25$ and $\delta = 0.4$. Phillips et al [2] prescribed somewhat more peaked current profiles and optimised the pressure profile. They found a slight, positive effect of triangularity. It is obvious that the different results concerning the effect of triangularity are due to the different ways of prescribing equilibrium profiles.

The main conclusions of the present study are easy to formulate. For *broad* pressure profiles, triangularity has little effect on the beta-limit. For *peaked* pressure profiles, triangularity has a clear positive effect, and $\delta \geq 0.4$ is highly favourable. To confine strongly peaked pressure profiles with high beta, the q-profile must have sufficient shear in the central region for local stability. The necessary central current gradients decrease with increasing triangularity. The current profiles for highly triangular cross-sections with $q_0 \geq 1$ and low q_s are considerably flatter than those maintained at steady-state in ohmic discharges, and will require non-inductive current drive.

ACKNOWLEDGEMENT

This study was performed under NET contract 310/88-7 FU CH NET, and was supported in part by the Fonds National Suisse pour la Recherce Scientifique. We are indebted to Dr. K. Borrass for many helpful discussions, in particular, concerning the importance of peaked pressure profiles.

REFERENCES

[1] TROYON, F., GRUBER, R., SAURENMANN, H., SEMENZATO, S., SUCCI, S., Plasma Phys. Controlled Fusion **26** (1984) 209.

[2] PHILLIPS, M.W., TODD, A.M.M., HUGHES, M.H., MANICKAM, J., JOHNSON, J.L., PARKER, R.R., Nucl. Fusion, **28** (1988) 1499.

[3] ROY, A., TROYON, F., in Theory of Fusion Plasmas, Proc. workshop, Chexbres, October 1988 (Editrice Compositori, Bologna 1989), p 175.

[4] "Next European Torus Status Report", NET report 51, Dec. 1985.

[5] GRUBER, R., TROYON, F., BERGER, D., et al, Comp. Phys. Comm., **21** (1981) 323.

[6] YASSEEN, F., COOPER, W.A., TURNBULL, A.D., TROYON, F., ROY, A., "MHD stability analysis for NET and INTOR", LRP 333/87, CRPP, Ecole Polytechnique Fédérale de Lausanne, Dec. 1987 (NET report 83).

[7] MIKHAILOVSKII, A.B., SHAFRANOV, V.D., Zh. Eksp. Teor. Fiz. **66**, (1974) 190 [Sov. Phys. JETP **39** (1974) 88]. See also review by WESSON, J.A., Nucl. Fusion, **18** (1978) 87.

[8] TURNBULL, A.D., SECRETAN, M.A., TROYON, F., SEMENZATO, S., GRUBER, R., J. Comp. Phys. **66** (1986) 391.

[9] HOGAN, J., "Linear ideal MHD stability calculations for ITER", presented at the ITER workshop on operational limits, IPP Garching, June 1988.

[10] FREIDBERG, J.P., Rev. Mod. Phys. **54** (1982) 801, and references therein.

[11] MANICKAM, J., POMPHREY, N., TODD, A.M.M., Nucl. Fusion **27** (1987) 1461; HENDER, T.C., HAYNES, P.S., ROBINSON, D.C., SYKES, A., in Controlled Fusion and Plasma Physics (Proc. 14th Eur. Conf., Madrid 1987), Part 1, p. 231.

[12] TODD, A.M.M., MANICKAM, J., OKABAYASHI, M., GRIMM, R.C., GREENE, J.M., JOHNSON, J.L., Nucl. Fusion, **19** (1979) 743.

Figure 1 a

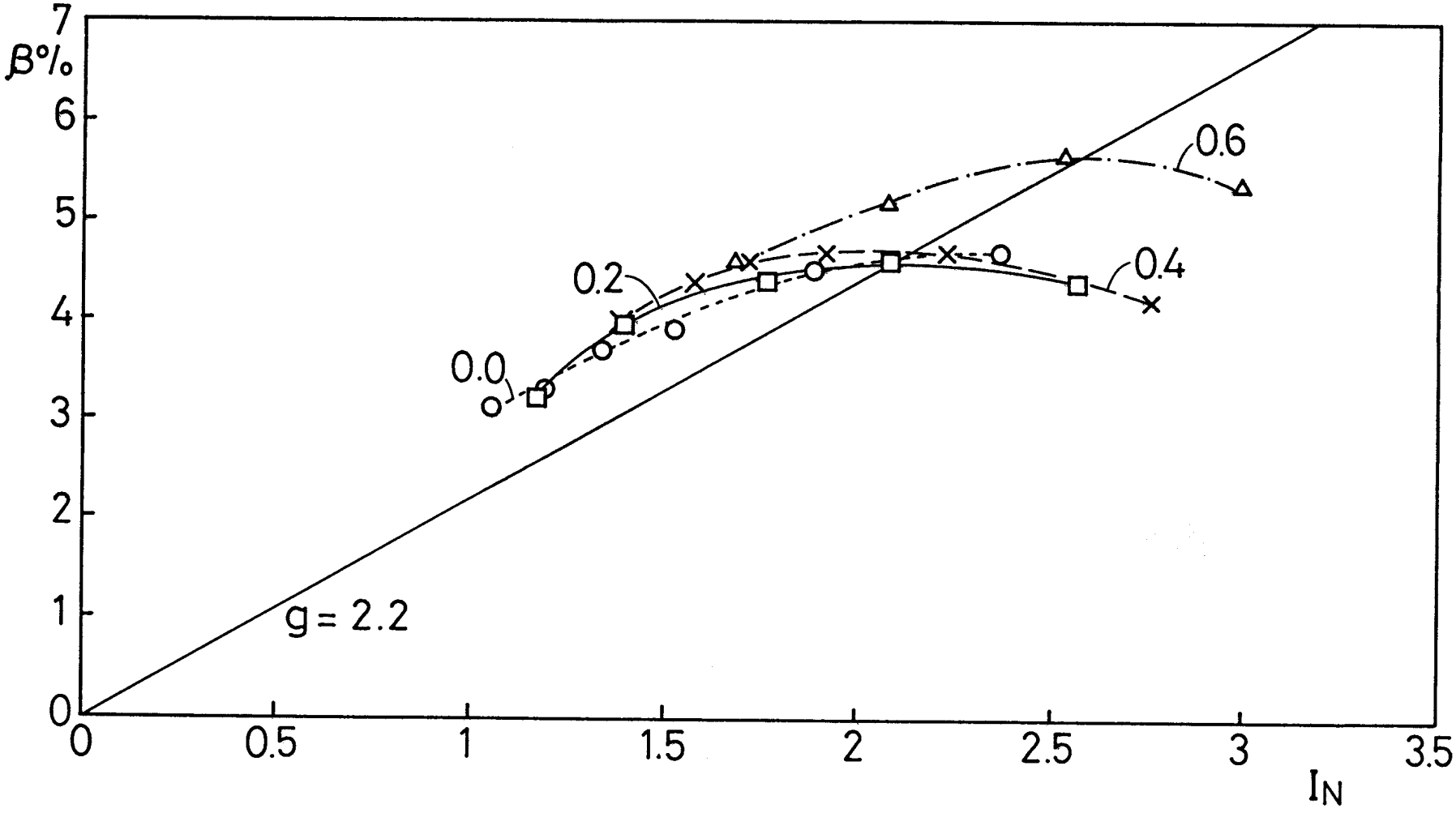

Figure 1 b

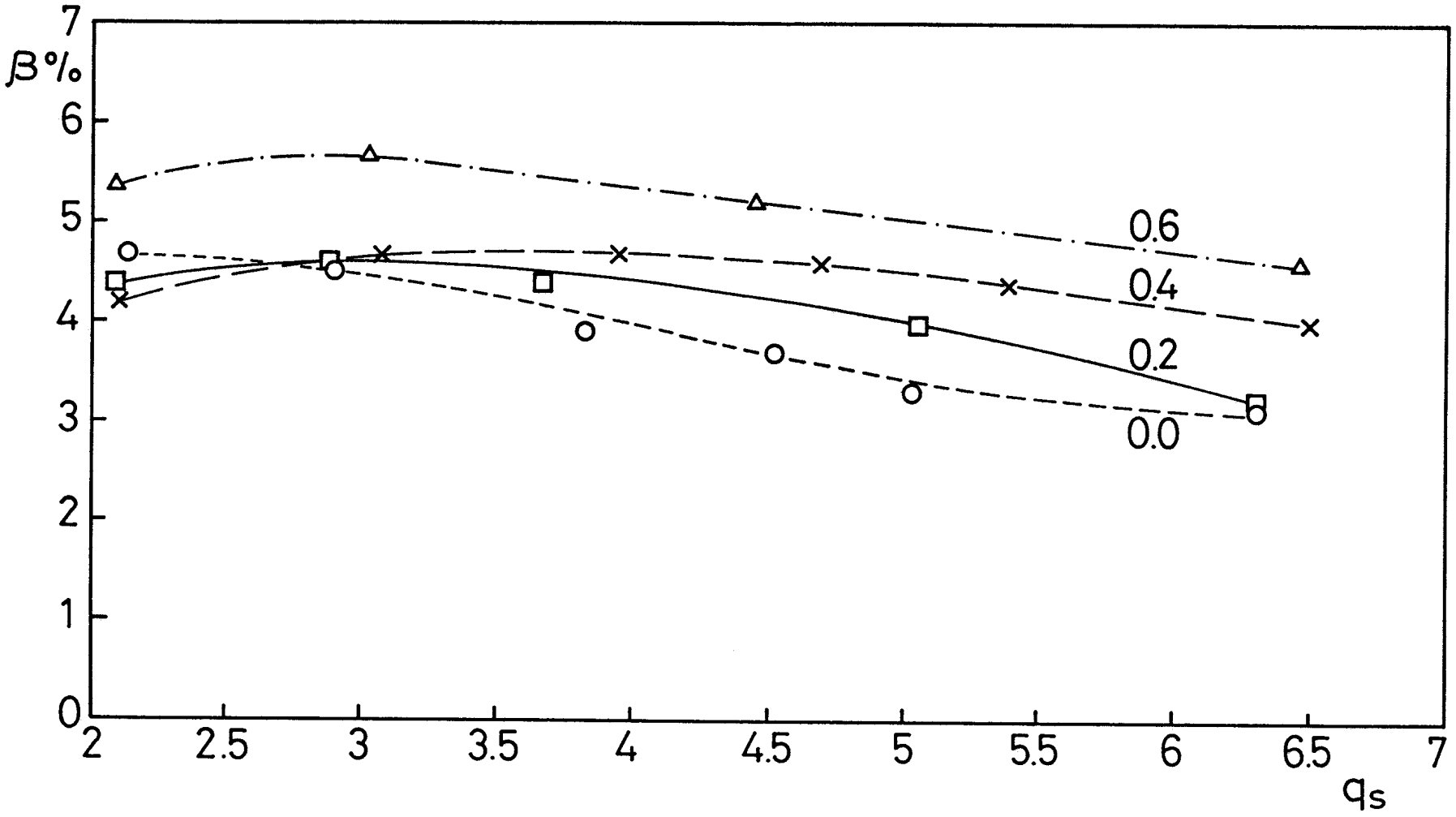

Figure 1 c

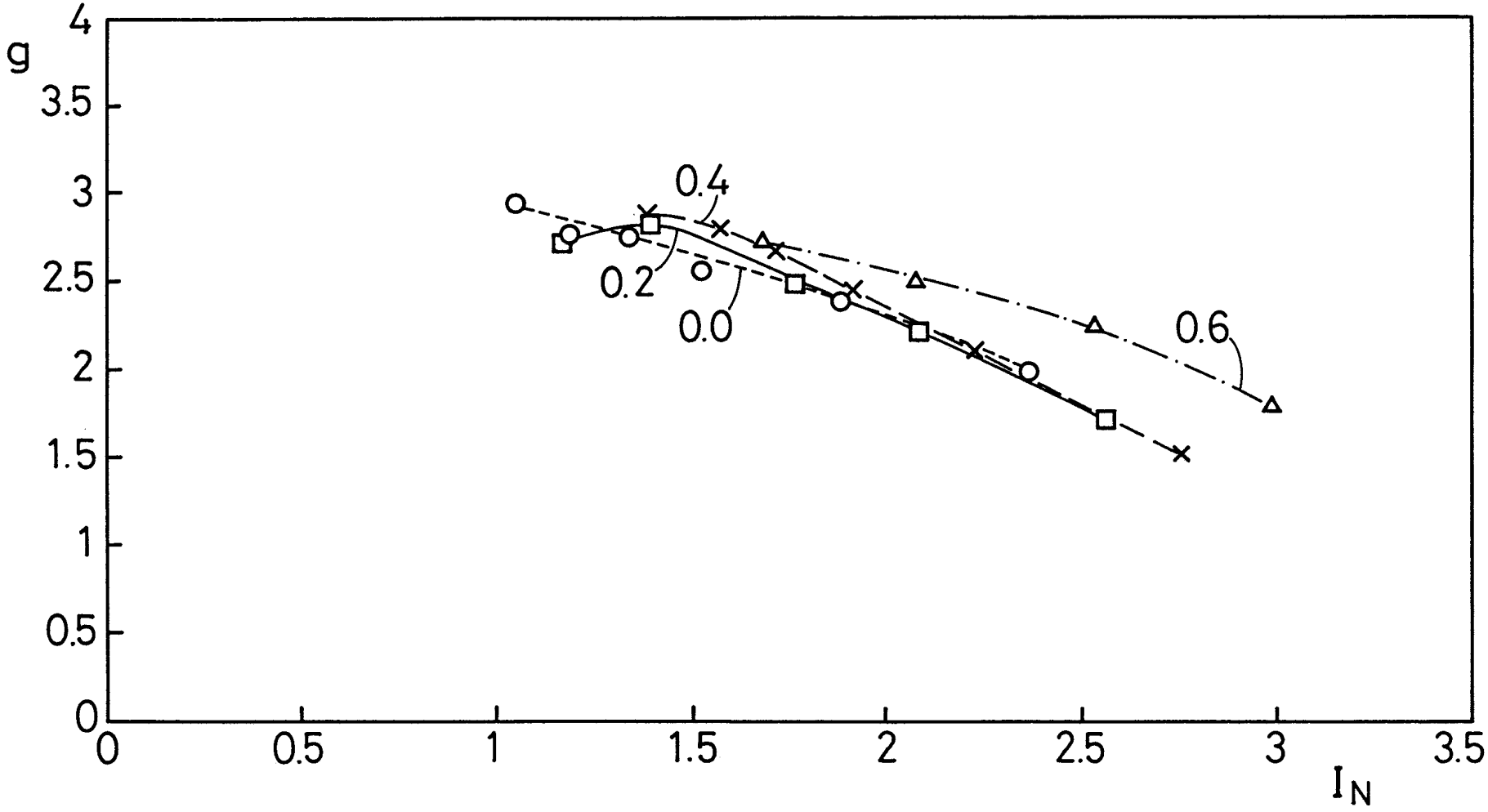

Figure 2

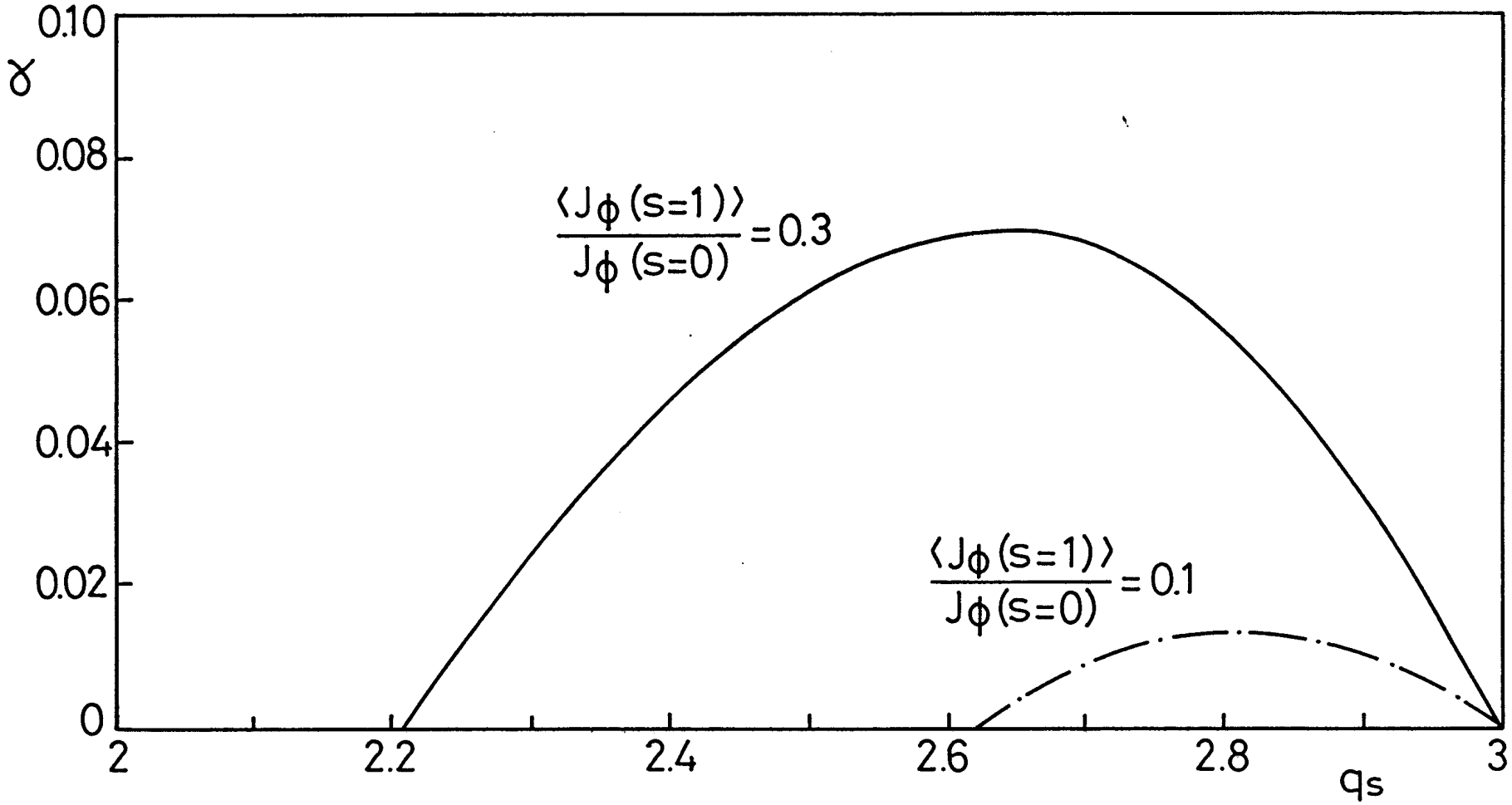

Figure 3 a

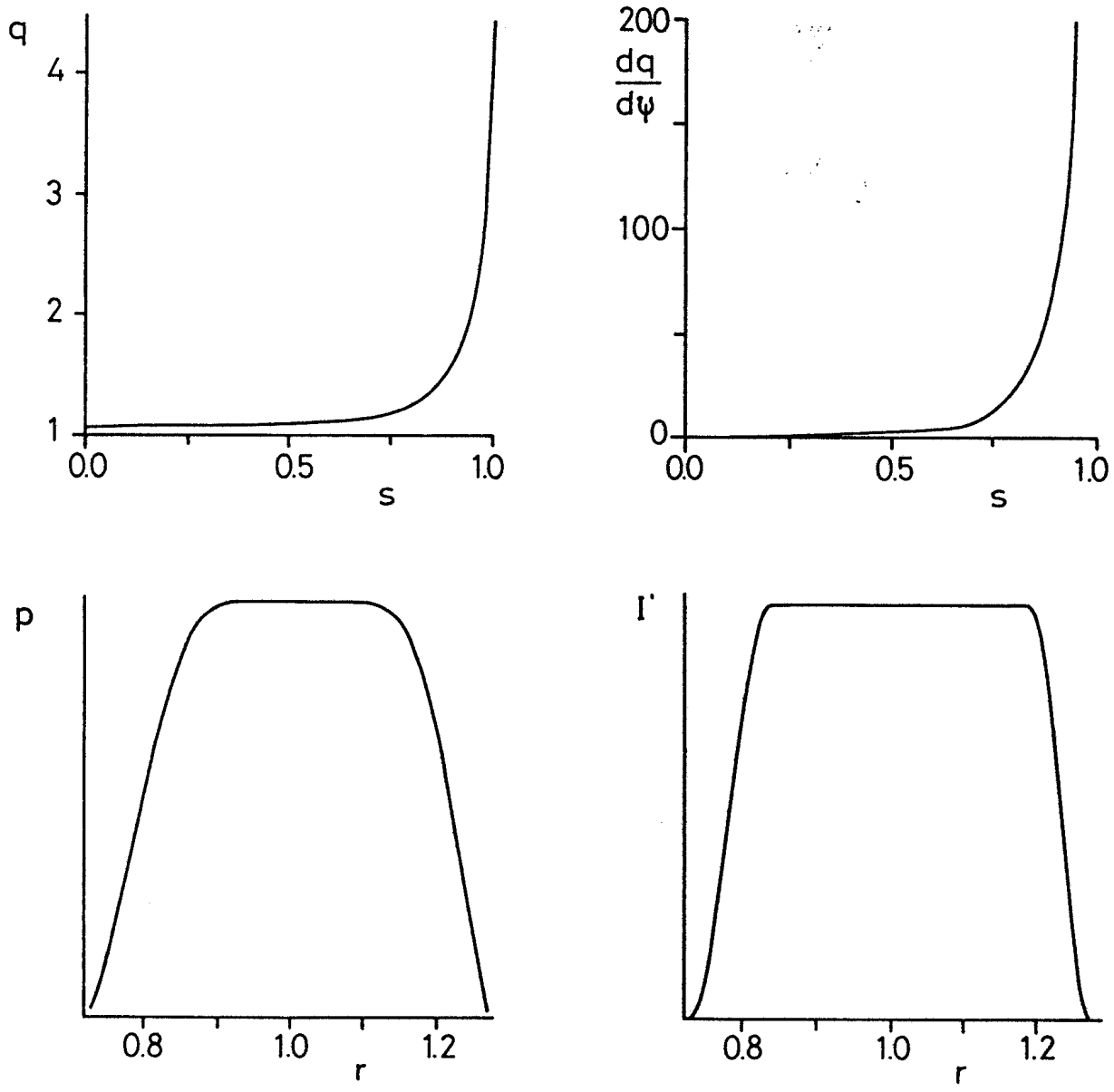

Figure 3 b

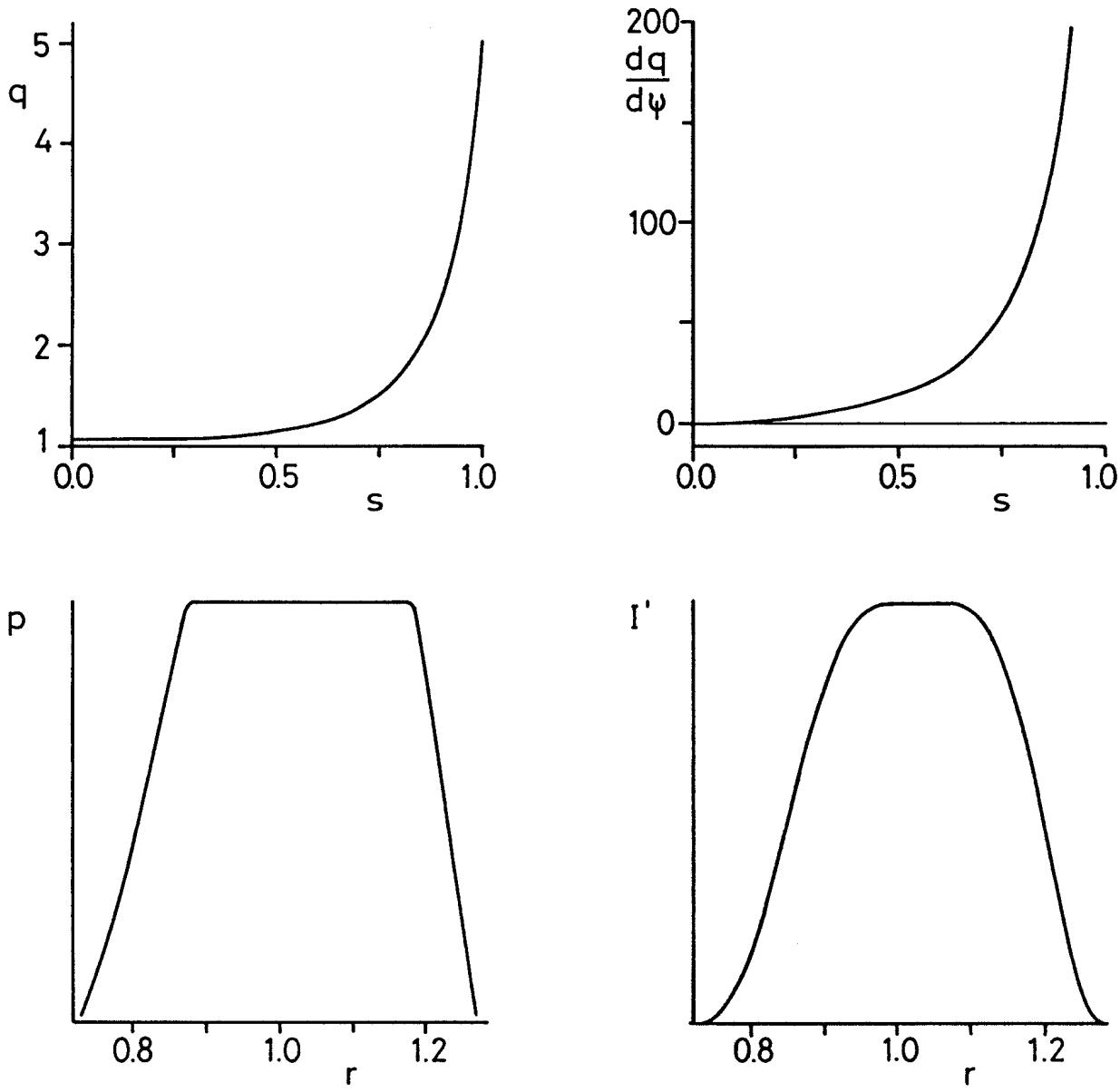

Figure 4

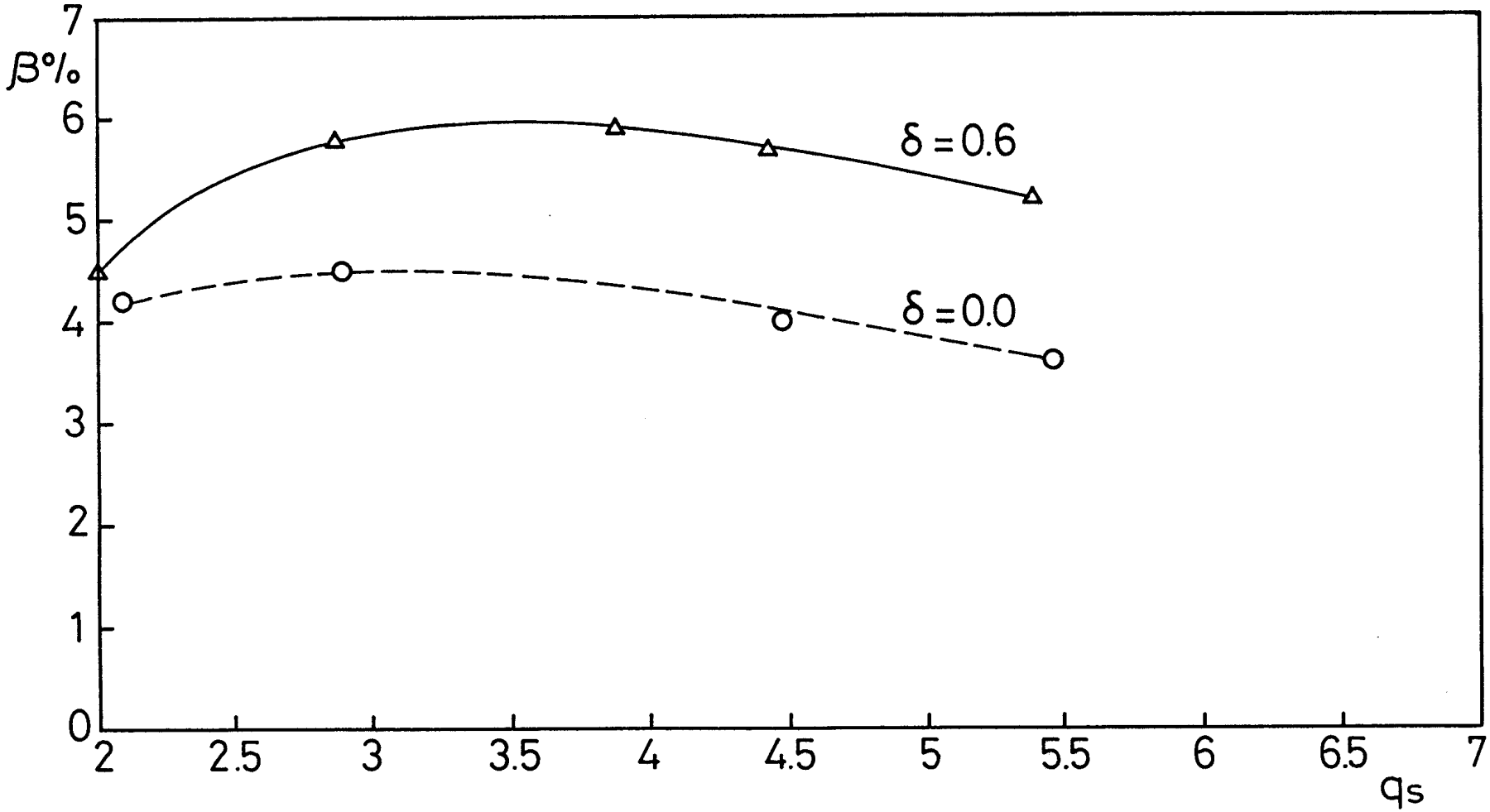

Figure 5 a

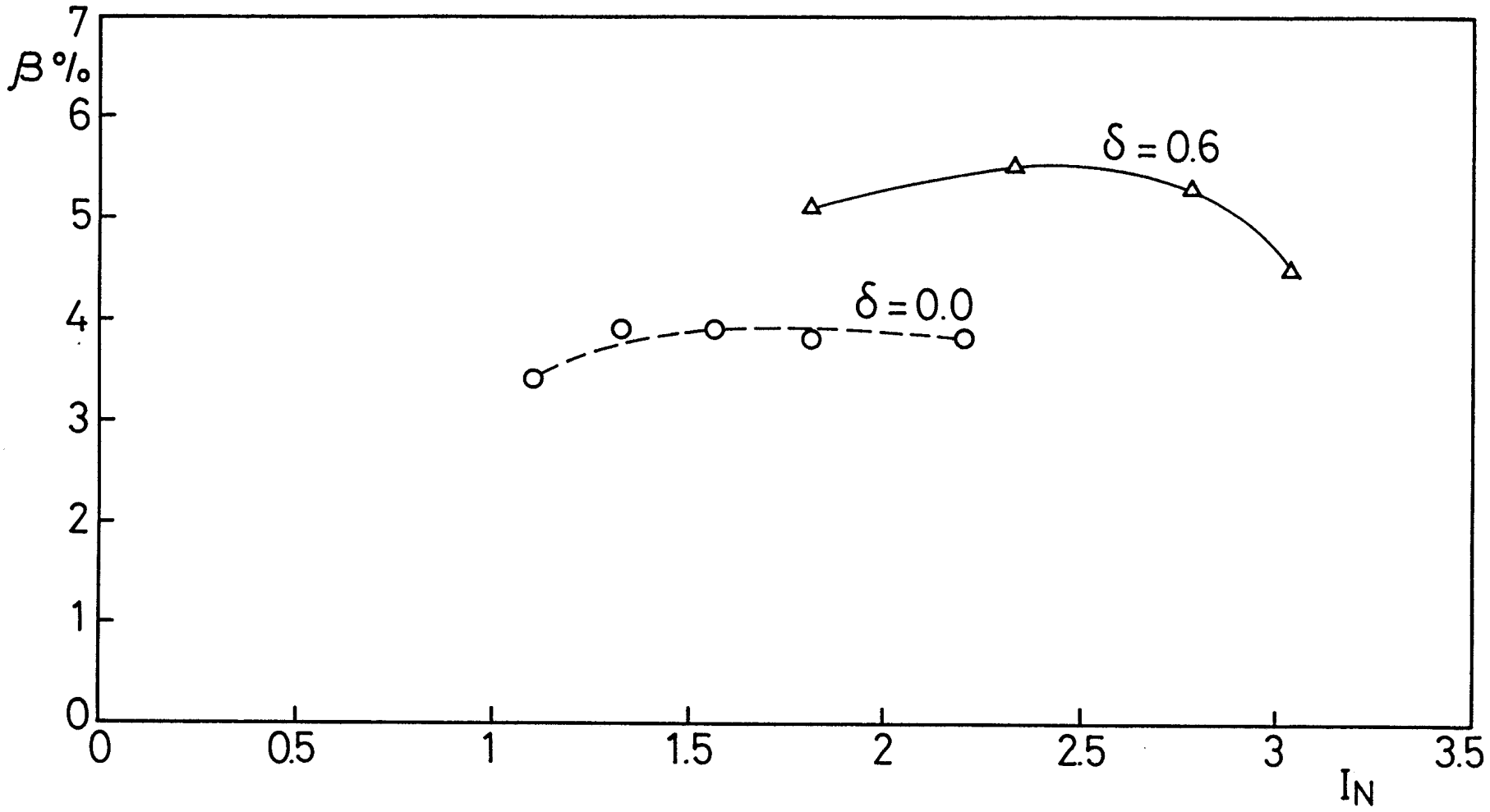

Figure 5 b

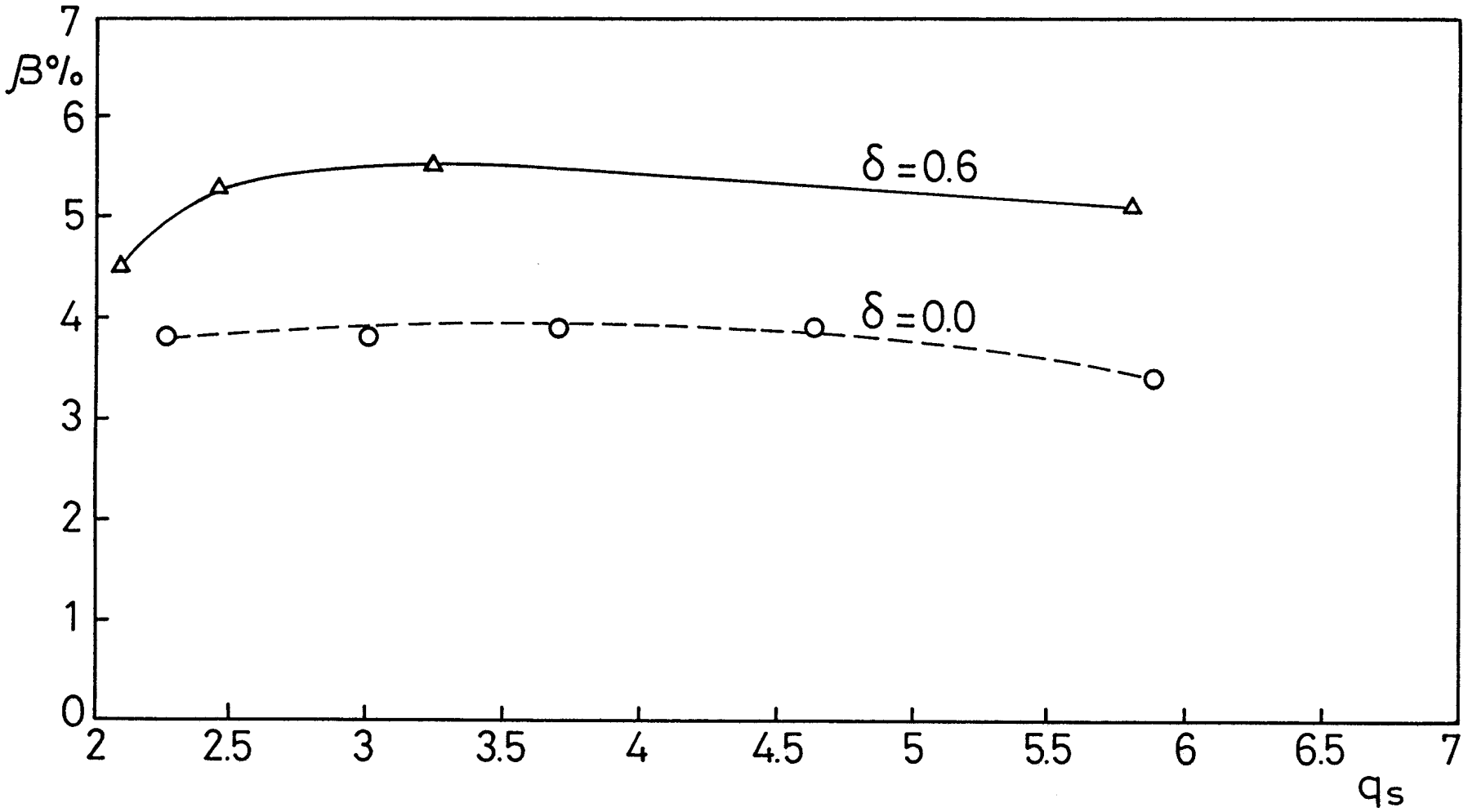

Figure 5 c

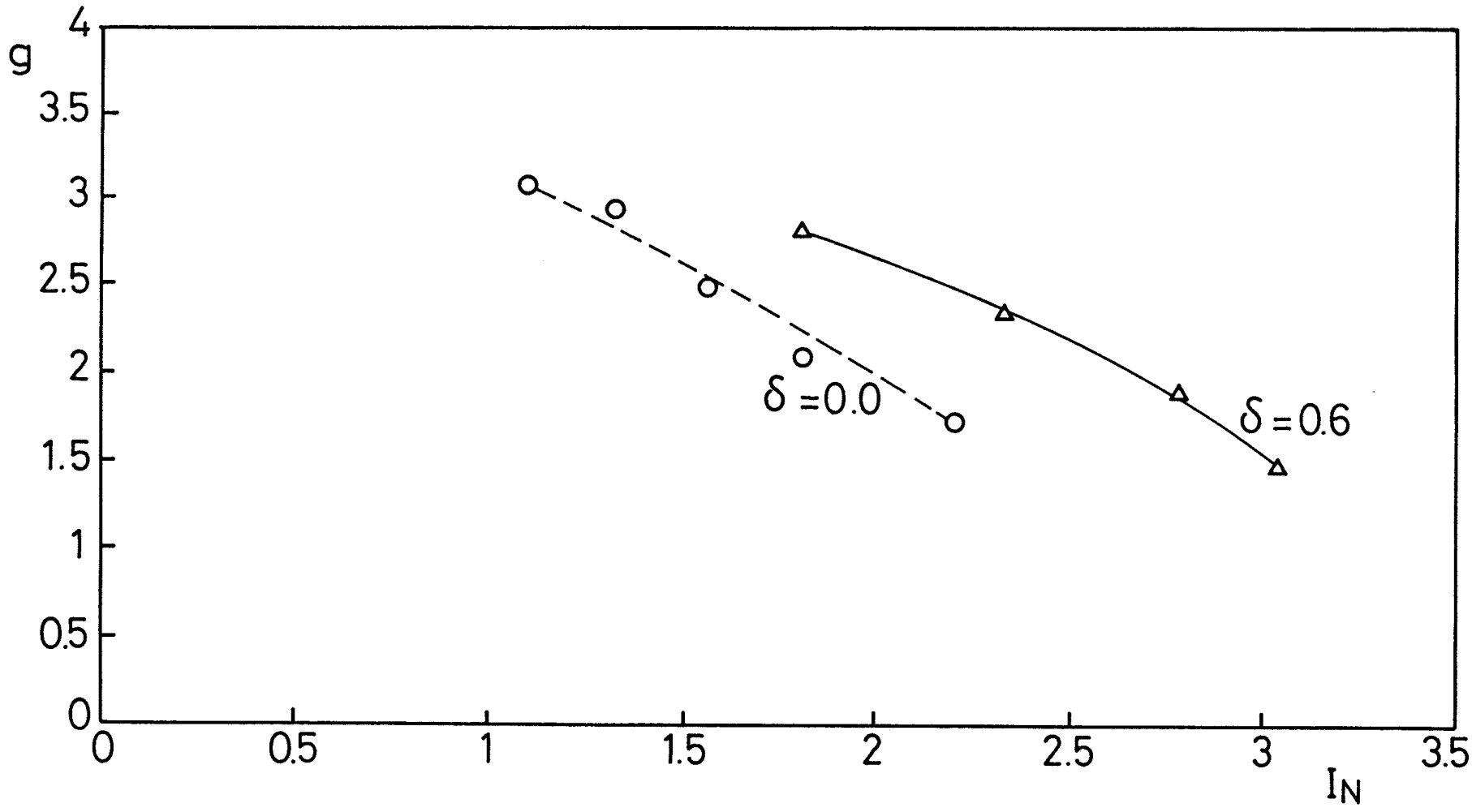

Figure 6 a

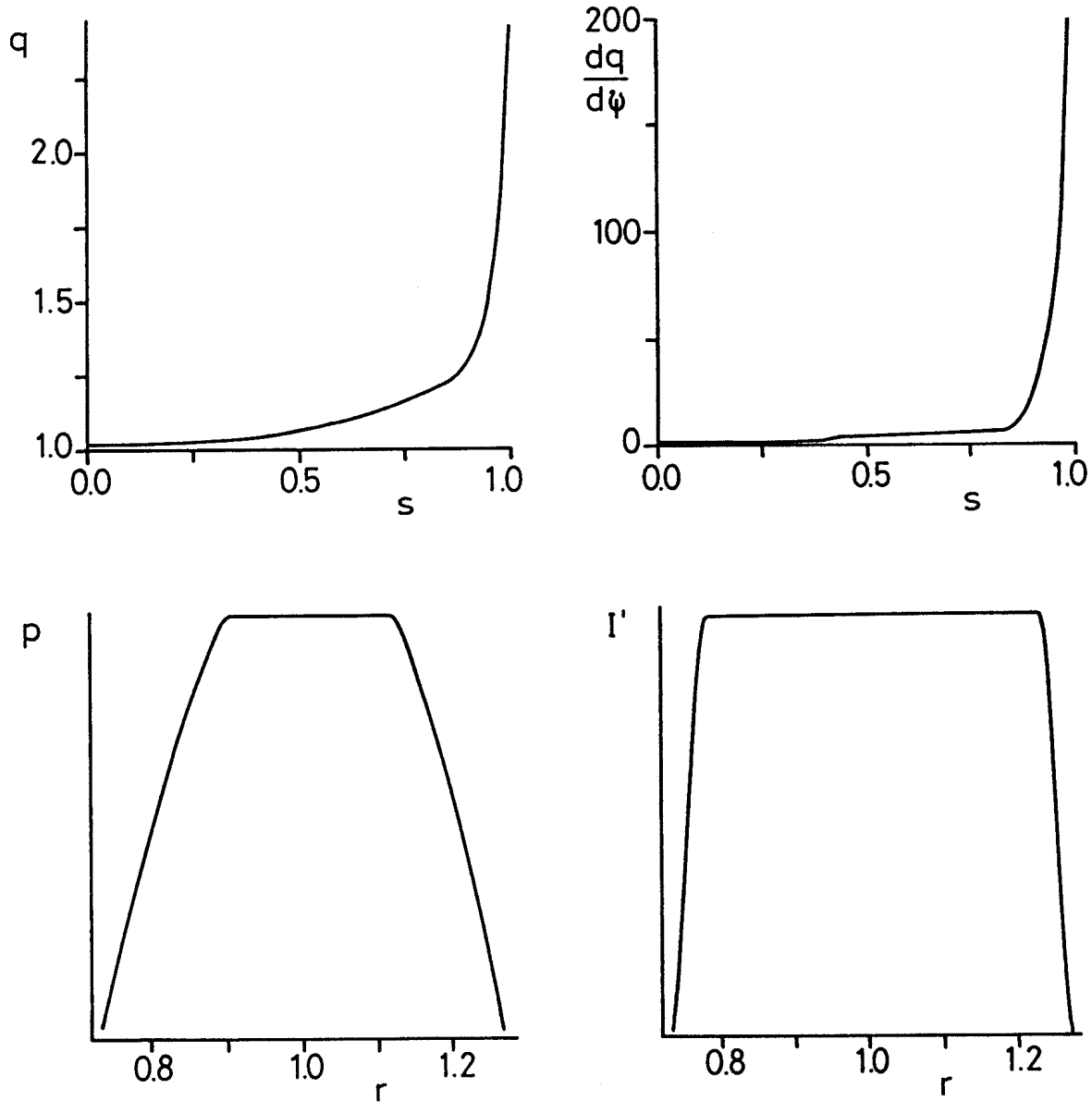

Figure 6 b

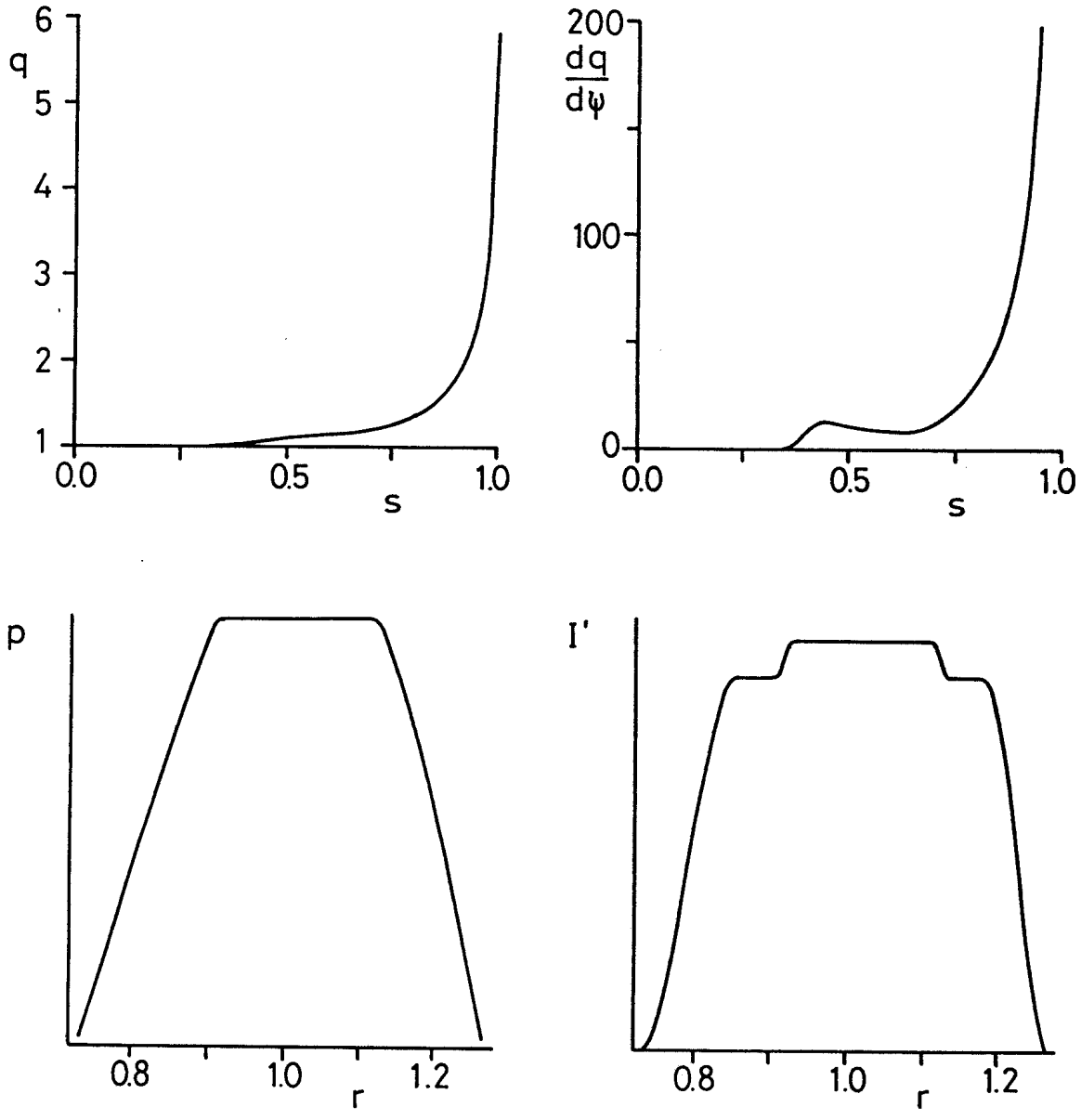

Figure 7 a

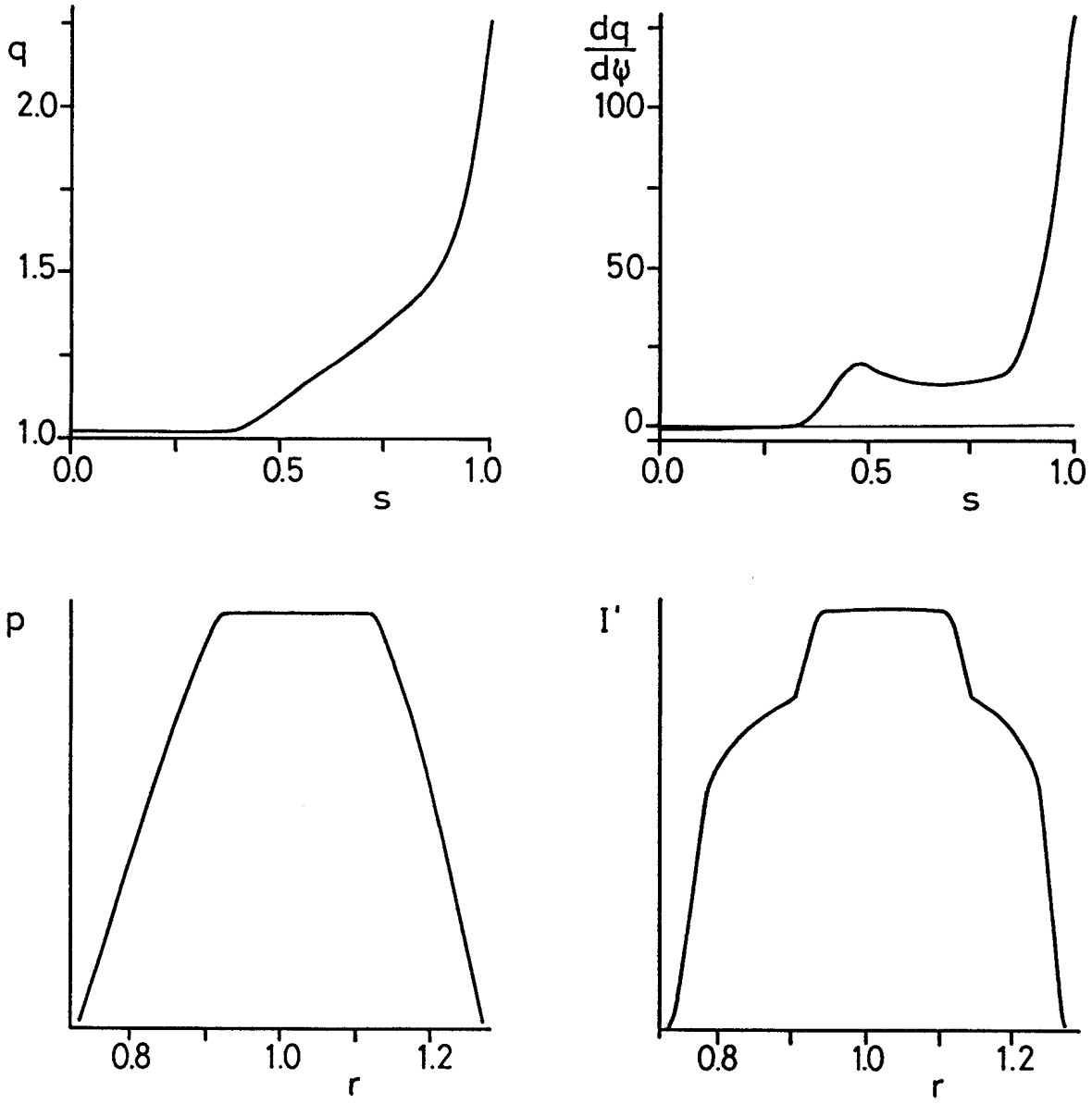

Figure 7 b

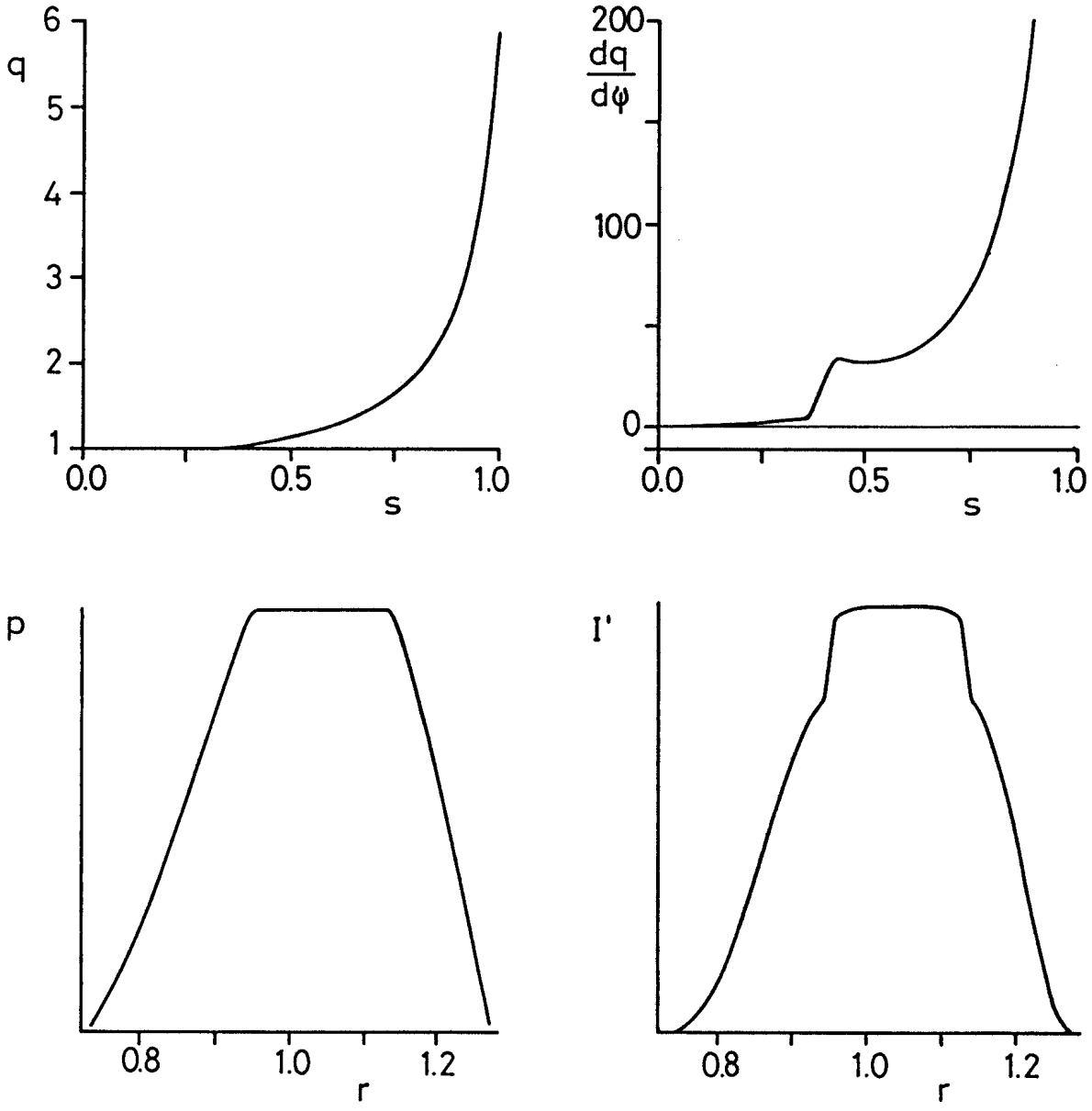

Figure 8 b

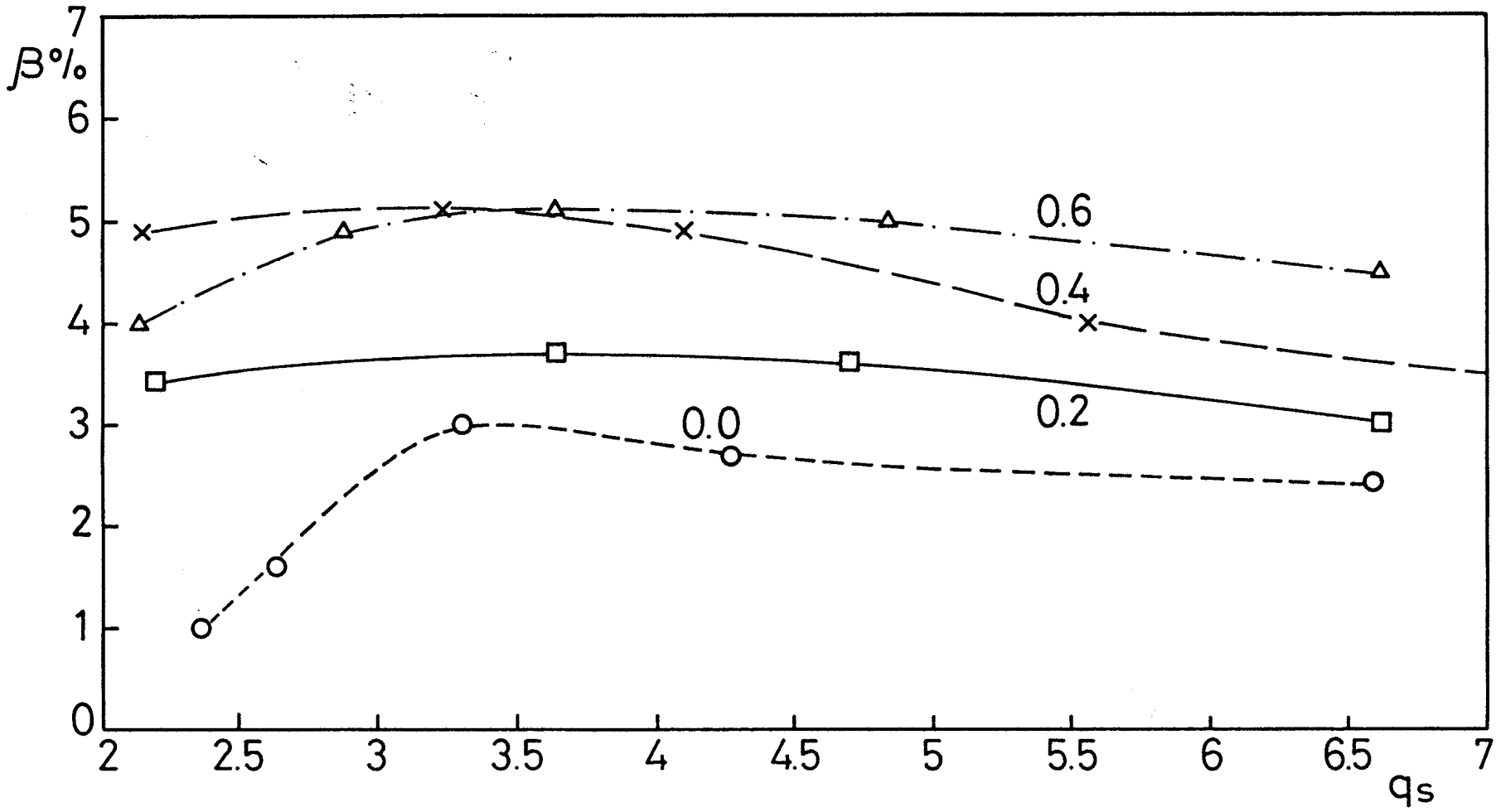

Figure 8 c

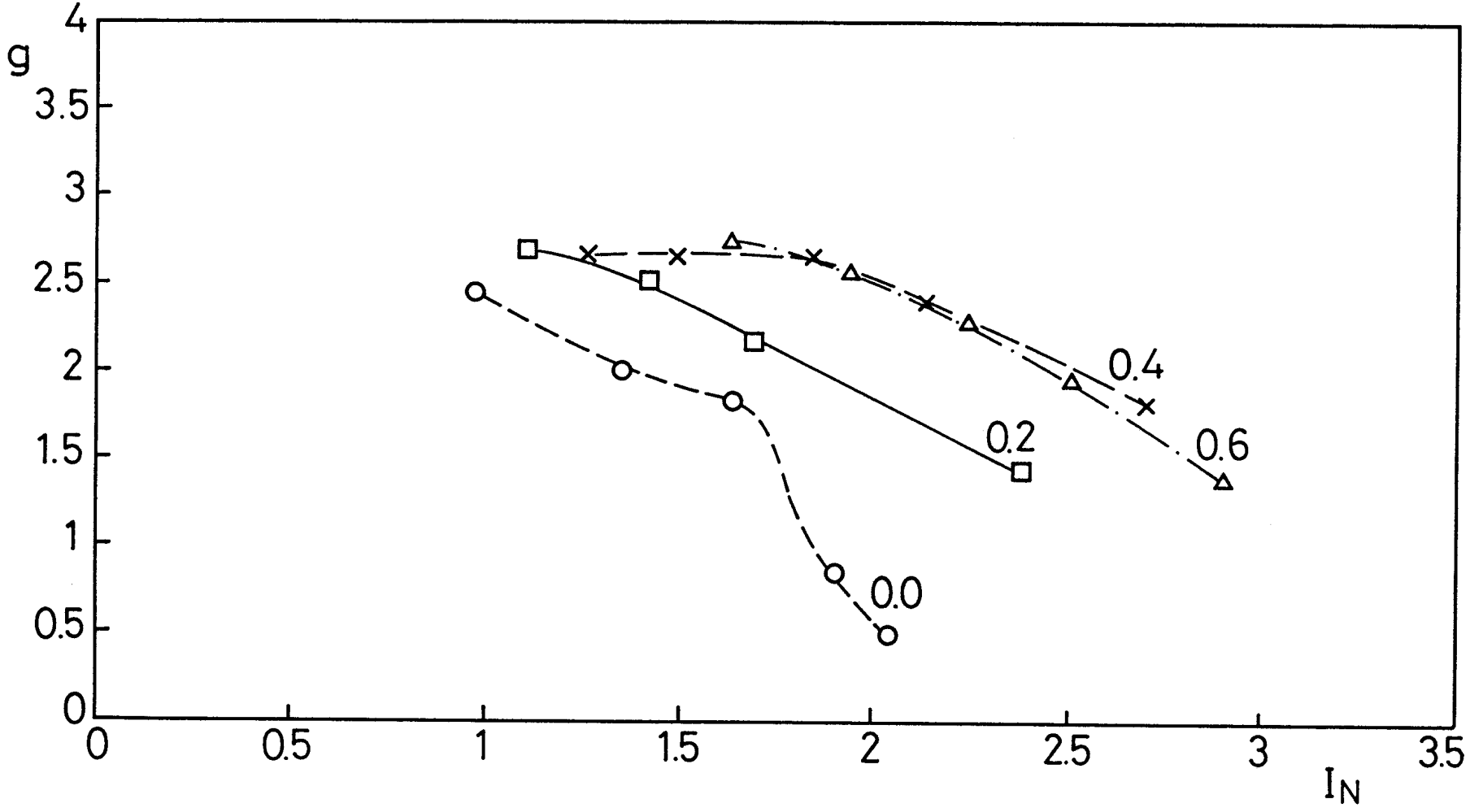

Figure 9 a

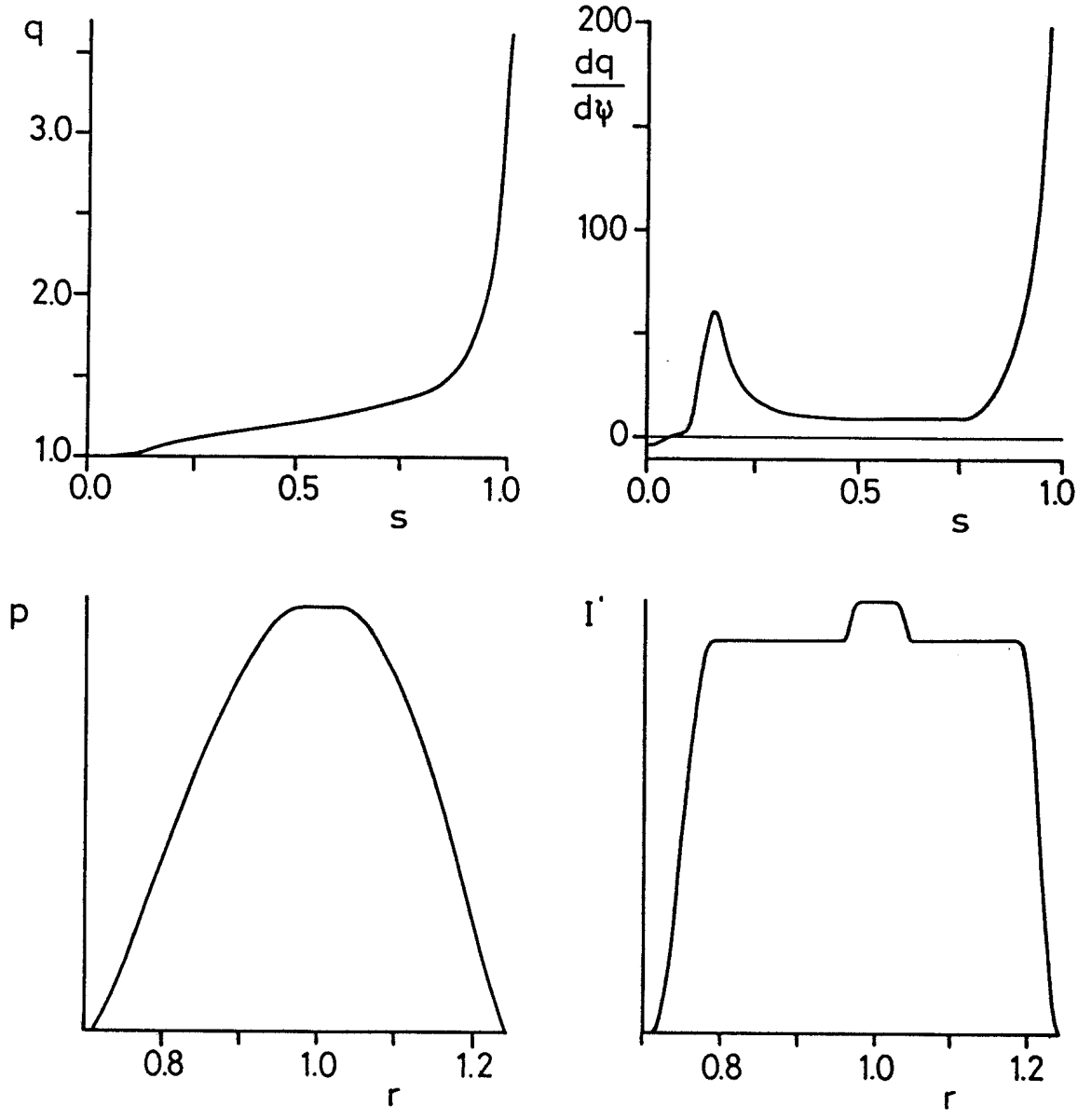

Figure 9 b

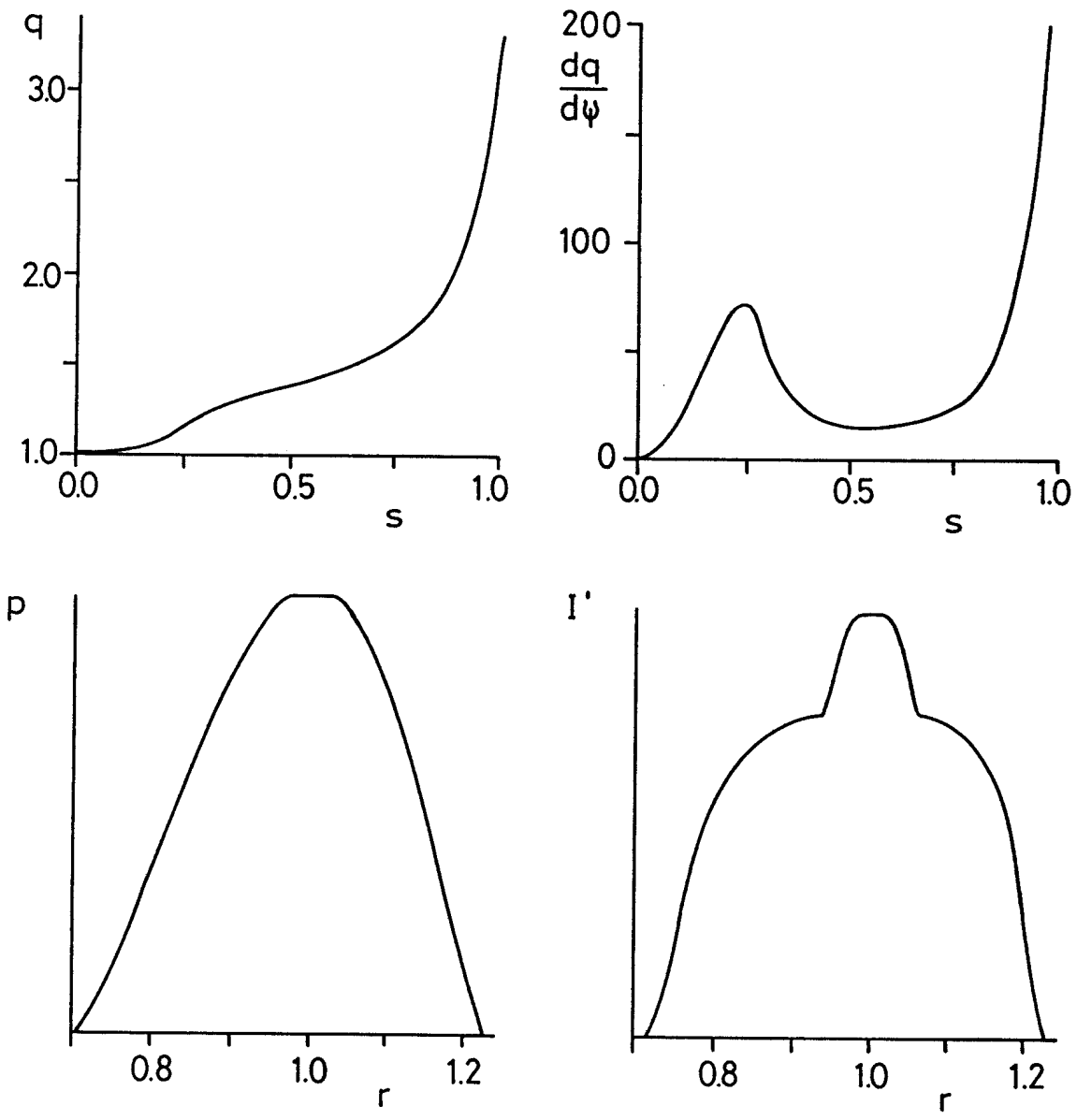

Figure 10 a

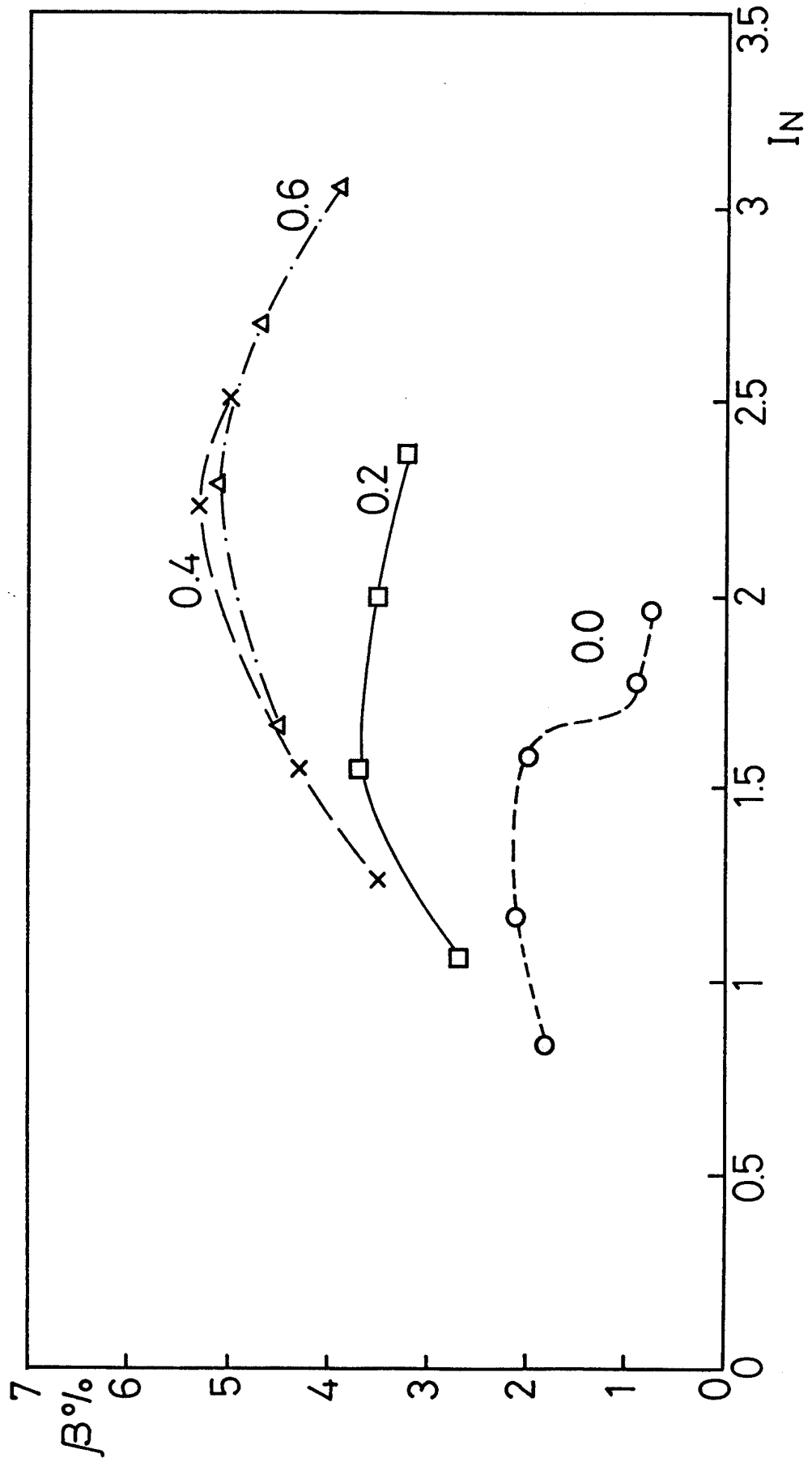

Figure 10 b

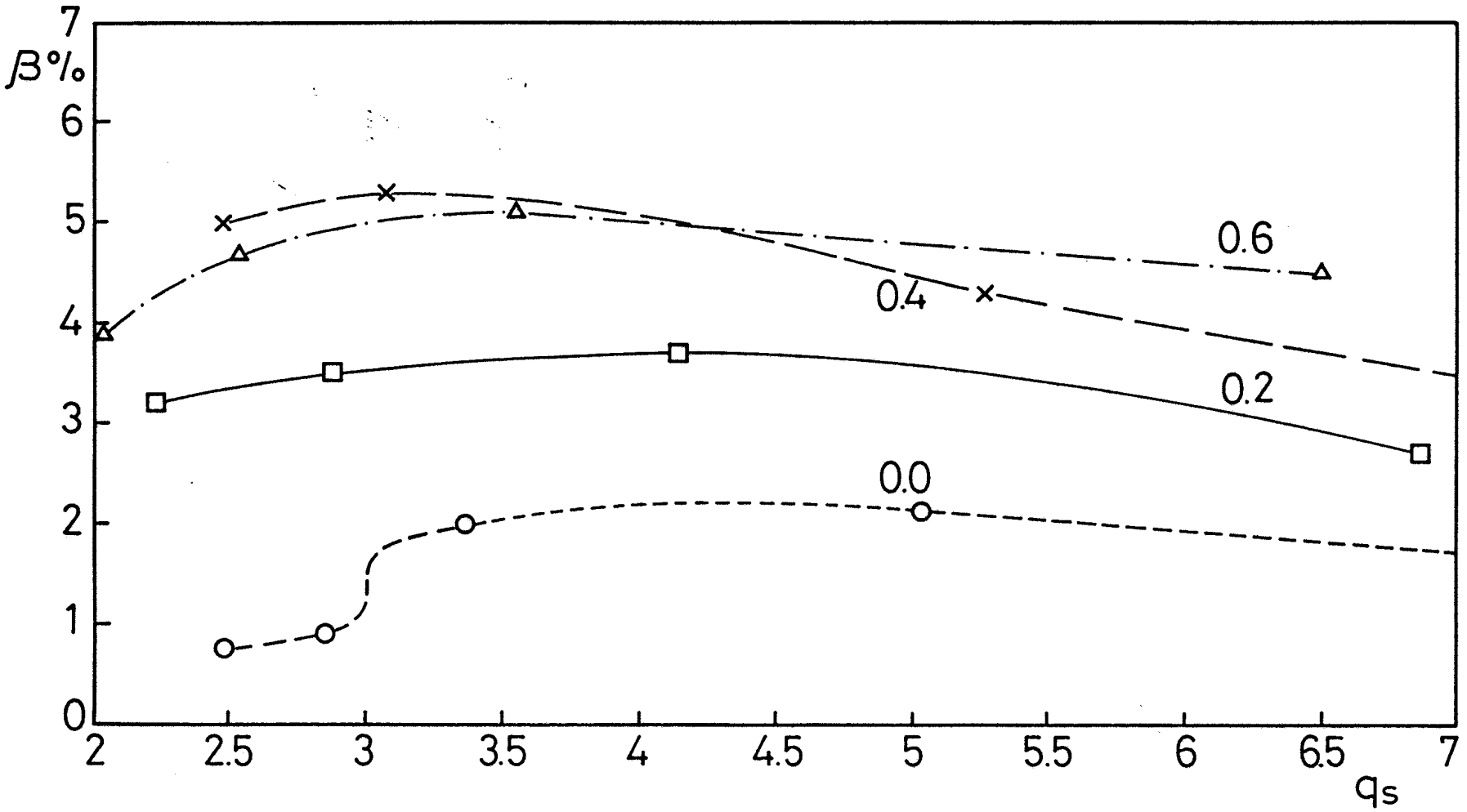

Figure 10 c